

THE FLORIDA STATE UNIVERSITY

COLLEGE OF ARTS AND SCIENCES

EMBEDDING LUMINESCENT NANOCRYSTALS IN SILICA SOL-GEL MATRICES

by

LINDSEY MICHELLE SORENSEN

A Thesis submitted to the  
Department of Chemistry and Biochemistry  
in partial fulfillment of the  
requirements for the degree of  
Masters of Science

Degree Awarded:  
Spring Semester, 2006

Copyright © 2005  
Lindsey Sorensen  
All Rights Reserved

The members of the committee approve the thesis of Lindsey Sorensen defended on December 1, 2005.

---

Geoffrey F. Strouse  
Professor Directing Thesis

---

Albert E. Stiegman  
Committee Member

---

William T. Cooper  
Committee Member

Approved:

---

Naresh Dalal, Chair, Department of Chemistry and Biochemistry

The Office of Graduate Studies has verified and approved the above named committee members.

To my husband...I look forward to being a slacker again. Tmnt.

## ACKNOWLEDGEMENTS

I would like to thank the Air Force Institute of Technology for sending me on this assignment and the FSU Chemistry and Biochemistry Department for being willing to work with my compressed schedule and strange requests. Thank you to the FSU AFROTC Detachment 145 for being my only link to the military while here at school. Thank you to Melissa, Carole, and the Stiegman research group for teaching me about sol-gels, showing me instruments, and letting me steal supplies. Thank you to my wise research advisors for keeping me busy and creating the constant request for more aerogels. “Lindsey, could you make an aerogel that....”

To the ‘gentlemen’ of Room 503, thank you for keeping the day interesting, for adding their own comments to events, and for furnishing cake and champagne.

## TABLE OF CONTENTS

List of Figures .....	vii
List of Abbreviations .....	ix
Abstract .....	x
1. INTRODUCTION .....	1
1.1 The Problem .....	1
1.2 General Introduction .....	2
1.2.1 Introduction to Quantum Dots .....	2
1.2.2 General Sol-Gel Chemistry .....	3
1.3 Review of Literature .....	8
1.4 Summary of Chapters .....	9
2. XEROGEL SYNTHESIS .....	10
2.1 Chemical Preparation of Quantum Dot Sol .....	10
2.1.1 Sample Sol-Gel Procedure .....	11
2.1.2 Chemical Preparation of Synthesized Quantum Dot .....	11
2.1.3 Ligand Selection .....	11
2.1.4 Ligand Exchange Procedure .....	14
2.1.5 Creating a Gel .....	14
2.1.6 Gel Instabilities .....	17
2.1.7 Heat-treating Gels to Remove Solvent .....	20
2.2 Experimental Analysis of Xerogels .....	23
2.2.1 Photoluminescent Results .....	23
2.2.2 Acetonitrile Brightening .....	23
3. AEROGEL SYNTHESIS .....	28
3.1 Aerogel Introduction .....	28
3.1.1 Background .....	28
3.1.2 Applications .....	29
3.2 Synthesis and Analysis .....	29
4. CRITICAL POINT DRYING PROCEDURE FOR AEROGEL FORMATION .....	35
4.1 Critical Point Drying .....	35
4.1.1 Apparatus .....	35
4.1.2 Supercritical Point .....	35
4.1.3 Solvent Exchange .....	37
4.2 Instrument Use .....	38

4.2.1 Turning on Instrument .....	38
4.2.2 Venting and Supercritical Stages.....	39
4.2.3 Problem Solving.....	40
5. PRIMITIVE SENSOR EXPERIMENTS .....	41
5.1 Sensor Introduction.....	41
5.1.1 Electronic Noses.....	41
5.1.2 Nanomaterials as Environmental Sensors.....	41
5.2 CdSe Response to TNT .....	44
5.2.1 CdSe on Alumina Filter .....	42
5.2.2 CdSe in Xerogels.....	42
5.3 Recommendations for Further Explosive Sensor Research .....	43
6. CONCLUSIONS.....	45
6.1 Unanswered Questions.....	45
6.1.1 Xerogel.....	45
6.1.2 Aerogel.....	45
6.1.3 Sensors .....	46
6.2 Conclusions .....	46
REFERENCES.....	47
BIOGRAPHICAL SKETCH .....	50

## LIST OF FIGURES

1.1 Quantum dot luminescence under UV hand lamp. Illustrates correlation between size and emission .....	3
1.2 General sol-gel reaction.....	4
1.3 Sol-gel hydrolysis reaction .....	5
1.4 Sol-gel condensation reaction .....	5
1.5 Illustration of the sol-gel terminology .....	6
1.6 Pictorial representation of chemical reaction of a) liquid sol, b) alcogel, c) aerogel, and d) xerogel.....	7
2.1 General sol-gel reaction.....	10
2.2 Excitation and emission of a) 2.5 nm CdSe/ZnS, b) InP/ZnS, and c) 6 nm CdSe/ZnS parent dots used to xerogels and aerogels. ....	12
2.3 Picture of liquid gel after quantum dot solution has been added (left) and after gel has formed (right) .....	15
2.4 Three dishes showing progressing reaction. First (top-left) is TMOS solution only. The second (lower) is liquid sol-gel with quantum dot added before condensation. Finally the third (top-right) shows what happens when the reaction is too vigorous and quickly cracks.....	16
2.5 Two CdSe/ZnS xerogel monoliths prepared with identical quantum dot concentrations and conditions. Gel on left has spontaneously gone cloudy while gel on right is clear.....	18
2.6 Isotherm plots for BET of a) calcined and b) uncalcined InP xerogels.....	19
2.7 DSC-TGA data for uncalcined CdSe xerogel under a) oxygen and b) nitrogen gas flow.....	21

2.8 DSC-TGA data for a) pure CdSe quantum dot and b) blank xerogel both under nitrogen .....	22
2.9 Photo of approximately 3 mg of 2.5 nm CdSe/ZnS 5 cm diameter xerogel disk excited with 1 mW 488 nm laser and viewed through a 488 nm filter in a) room light and b) dark .....	24
2.10 Graph of normalized photoluminescence intensity of a dried CdSe/ZnS xerogel and parent dot solution .....	25
2.11 Photoluminescence of InP/ZnS xerogel and parent dot solution. Luminescence is very weak and impurity peak at 420 nm that originates from tin impurities in TMOS is evident. ....	26
2.12 Tracking of 2.5 nm CdSe/ZnS xerogel photoluminescence tracked over 24 hours as a) intensity b) maximum intensity tracked through time .....	27
3.1 Silica aerogel containing 2.5 nm CdSe/ZnS quantum dots .....	30
3.2 UV-Vis scan of 2.5 nm CdSe/ZnS aerogel .....	31
3.3 6 nm and 2.5 nm aerogels seen in room light and under 488 nm laser excitation as seen through a 488 nm filter. Luminescence seen in photo is from quantum dot emission .....	33
3.4 Photoluminescence of 2.5 nm parent dot solution and aerogel (red and yellow) as well as 6 nm parent dot solution and aerogel (green and blue). Peaks at 420 nm are tin impurity peaks from TMOS solution .....	34
4.1 Location of valves on critical point drying apparatus .....	36
4.2 Pressure-temperature phase diagram for CO <sub>2</sub> .....	37
4.3 Coolant control box of critical point dryer .....	39
5.1 Photoluminescence of 6 nm CdSe dots before and after TNT exposure and also after heating to remove TNT .....	43



## LIST OF ABBREVIATIONS

APAPES - Aminoethylaminopropyltriethoxysilane  
APS – 3- Aminopropyltrimethoxysilane  
APeS – 3-Aminopropyltriethoxysilane  
BET – Brunner Emmet Teller  
DSC/TGA – Differential Scanning Calorimeter – Thermogravimetric Analysis  
EtOH – Ethanol  
HDA – Hexadecylamine  
HPLC – High Pressure Liquid Chromatography  
LED – Light Emitting Diode  
MeOH – Methanol  
MPA – Mercaptopropionic Acid  
MPS – 3-Mercaptopropyltrimethoxysilane  
RDX – Rapidly Detonating Explosive  
SILAR – Successive Ionic Layer Adsorption and Reaction  
TEOS – Tetraethylorthosilicate  
TMOS – Tetramethylorthosilicate  
TNT – Trinitrotoluene  
TOP – Trioctylphosphine  
TOPO – Trioctylphosphine oxide  
QD – Quantum Dot  
UV-Vis – Ultraviolet-Visible

## ABSTRACT

We have synthesized stable, highly luminescent silica xerogels as well as optically transparent, stable aerogels that were embedded with 2.5 nm and 6 nm CdSe and 6 nm InP quantum dots. By capping the quantum dot with 3-aminopropyltriethoxysilane, a dot is able to condense within the structure of a forming silica gel. This network keeps the quantum dot in place during the solvent exchange procedure necessary to form low-density silica aerogels using supercritical drying procedures. The resulting aerogel networks show a high surface area of 789.7 m<sup>2</sup>/g and xerogels show a surface area of 448 m<sup>2</sup>/g, with a pore size of 3.16 nm. Materials created are stable under atmospheric conditions and up to temperatures of 150°C.

## CHAPTER 1

### INTRODUCTION

#### **1.1 The Problem**

This research starts at the beginning of a search for a novel functional material, truly concept development. There are several potential problems that could be addressed by further research of silica-embedded quantum dots. Sol-gel chemistry is well known and widely used for creation of glasses and ceramic materials. Semiconducting nanocrystals that exhibit three dimensional quantum confinements, known as ‘quantum dots,’ have found applications in various optical materials. Combining these two branches of research could help create new materials to replace environmentally unsafe solid-state lighting components. The fluorescent bulbs ubiquitous in global business environments combine mercury vapor in an inert gas and electricity to produce plasma, emitting photons of a very short wavelength. This short ultraviolet light excited a combination of phosphors in the bulb, producing white light. Each time a bulb is broken and especially during disposal the mercury vapor is released into the atmosphere, harming the health of surrounding humans. Mercury exposure causes severe health complications [1]. The search for a cost-efficient and environmentally friendly alternative to traditional phosphors highlights the interest in placing these highly efficient luminescent particles in a stable material.

A multitude of research is currently being performed that looks to see if different semiconducting nanocrystals have the properties sufficient for such applications [2-5]. Mercury-free lighting as well as Light Emitting Diodes (LED) requires phosphors that are excited between 360 and 450 nm. In order to compete with current technology, the efficiency of the excitation should be very high, heat generated by inefficient excitations low, stability of phosphor high, and

finally cost of generating phosphor very inexpensive all to compete with currently used technology.

Embedding a semiconductor in a porous, inert material creates possibilities for various sensor technologies. By varying the molecule bound to the exterior of the quantum dot, you can alter the chemistry at which luminescence from an incoming photon would be quenched by the material for which you are sensing

## 1.2 General Introduction

Everyday, human desire to understand and master our surroundings brings new and revolutionary scientific breakthroughs. The quest for knowledge described in this thesis attempts to successfully merge the new field of semiconductors exhibiting quantum confinement [6] and a centuries old process of silica formation from liquid components [7]. The merger of these two research fields has the potential to impact the field of solid-state lighting by usurping fluorescent bulbs as the powerhouse of lighting.

### 1.2.1 Introduction to Quantum Dots

A quantum dot is a special class of inorganic materials. These materials are nanocrystalline inorganic solids that are smaller in diameter than the Bohr radius for that molecule. Excitation energy greater than the band gap promotes an electron into the conduction band and a positively charged hole is left in the valance band. Both have charge, mass, and velocity and when the two recombine, a photon of light is released. The approximate spatial separation, the Bohr radius in analogy to the hydrogen atom, of the two charged particles has been estimated to be between 1 nm and 10 nm in size for an average semiconductor system but larger sizes can be seen depending on the electron/hole mass of the system [8]. Semiconductors that are smaller than the Bohr radius in size are referred to as ‘quantum dots’ for the unique optical properties that they possess. Since the size of the nanocrystal is around the distance that an electron and hole can travel, the quantum properties can be described by a particle in a box. Specifically, the Brus model can describe the energy gap of a quantum dot as follows:

$$E_g (\text{quantum dots}) = E_g (\text{bulk}) + (\hbar^2/8R^2)(1/m_w + 1/m_h) - 1.8e^2/4\pi\epsilon_0\epsilon R \quad [8]$$

Where  $h$  is Planck's constant,  $R$  is quantum dot radius,  $m_e$  is the effective mass of the electron,  $m_h$  is the effective mass of the hole,  $\epsilon$  is the dielectric constant of the solid. This works well for larger quantum dot size but does not effectively predict band gap in smaller quantum dots.

Figure 1.1 illustrates the size dependence of the quantum dots. A nanocrystal of larger diameter has a lower energy of emission. If there are defects in the lattice, such as vacancies or impurities, the electron and hole can get 'trapped.' Once these trapped states recombine their energy has been lowered and the photoluminescence released is shifted from optimal. In this way you can judge the purity of a synthesis by the symmetry of the photoluminescence peak. Peak asymmetry or a large red tail on a spectrum shows these trap emissions.

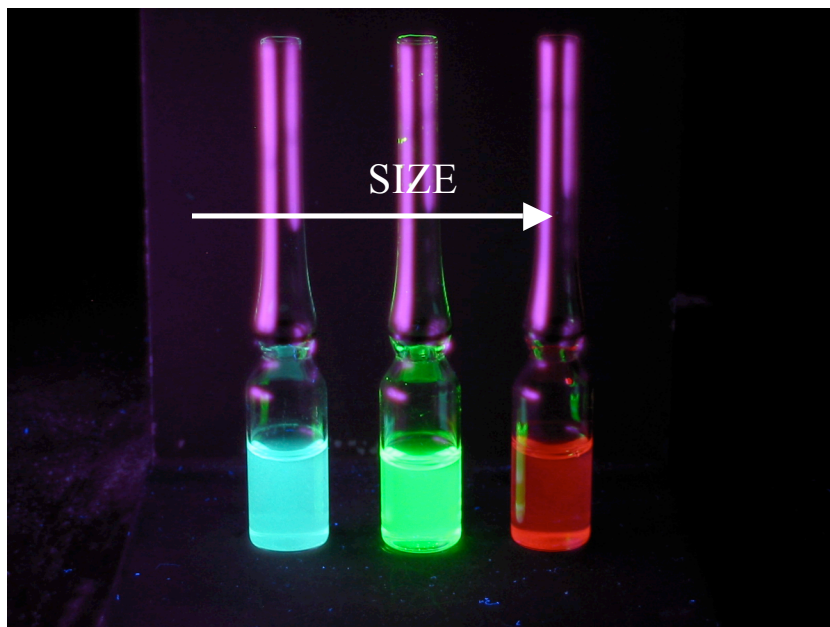


Figure 1.1 - Quantum dot luminescence under UV hand lamp. Illustrates correlation between size and emission.

### 1.2.2 General Sol-Gel Chemistry

The study of the sol-gel process dates back to the late 19<sup>th</sup> century. The term 'sol' comes from 'solution' and shows that the process begins as a suspension of colloids in a liquid solvent. As the colloid begins to polymerize and increase in length, the viscosity of the resulting liquid is drastically reduced until a three dimensionally connected network, or 'gel' forms.

The general reaction for a silica sol-gel reaction is as follows:

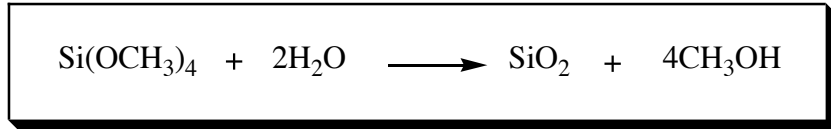


Figure 1.2 – General sol-gel reaction

There are two steps to producing the three dimensional network of silica. Hydrolysis (Figure 1.3) of the oxygen atoms bound to silicon turns them into an alcohol. Condensation (Figure 1.4) brings together two silica alkoxy molecules and removes water.

As the reaction progresses, each side of the tetrahedral formed around silica becomes connected through oxygen to another silicon atom and forms a three dimensional network. This network is by no means ordered on a long-range scale and is best described as possessing an order as described for an amorphous glass. After the gel has formed and is completely aged to let all available bonds connect, it sits in a solution of alcohol solvent and water used as a catalyst. The starting material used in the previous formulas is tetramethoxysilane (TMOS) but other silica alkoxy precursors can be used such as tetraethyloxysilane. The two precursors differ by reaction kinetics and alcohol solvent, and the choice of which to work with will vary according to the resulting product desired. Also sol-gel refers only to the general network of metal atoms that are interconnected and porous. Silicon need not be the interconnected metal but is the most commonly studied sol-gel matrix.

With this gel, a number of solid products can be formed that depend on how the solvent is removed from this fragile network. For definition and clarification purposes, the terminology used in this thesis is as follows and can be seen in Figures 1.5 and 1.6:

“Sol” – (Figure 1.6a) The solution of various reactants that are undergoing hydrolysis and condensation reactions. While the ‘sol’ can be quite viscous, it is still in its liquid form.

“Alcogel” – (Figure 1.6b) Comes from ‘alcohol-gel.’ Once the sol has formed three-dimensional networks that span the dimensions of the container holding the liquid it becomes too viscous to flow and is now solid. The gel is still impregnated with the alcohol and water solvents.

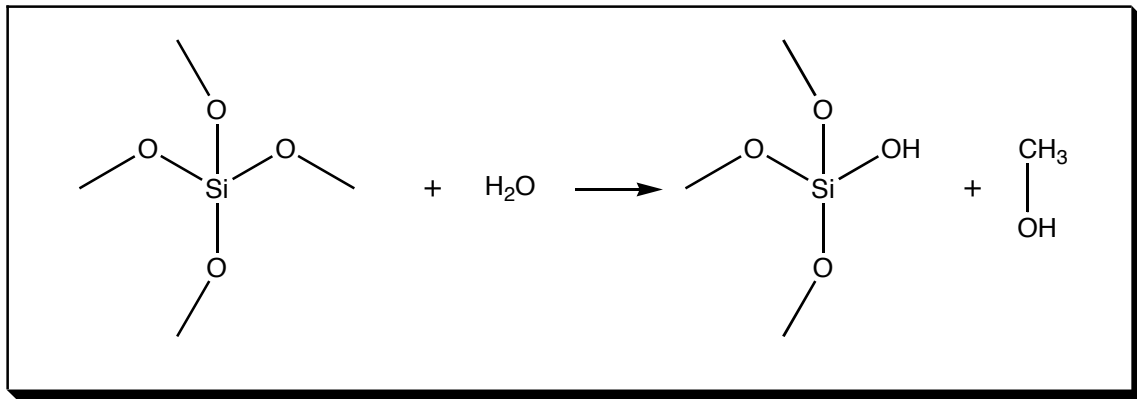


Figure 1.3: Sol-gel hydrolysis reaction

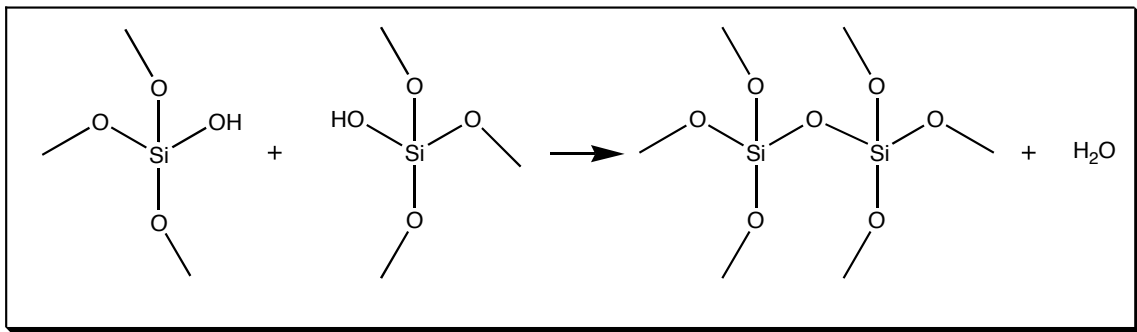


Figure 1.4: Sol-gel condensation reaction

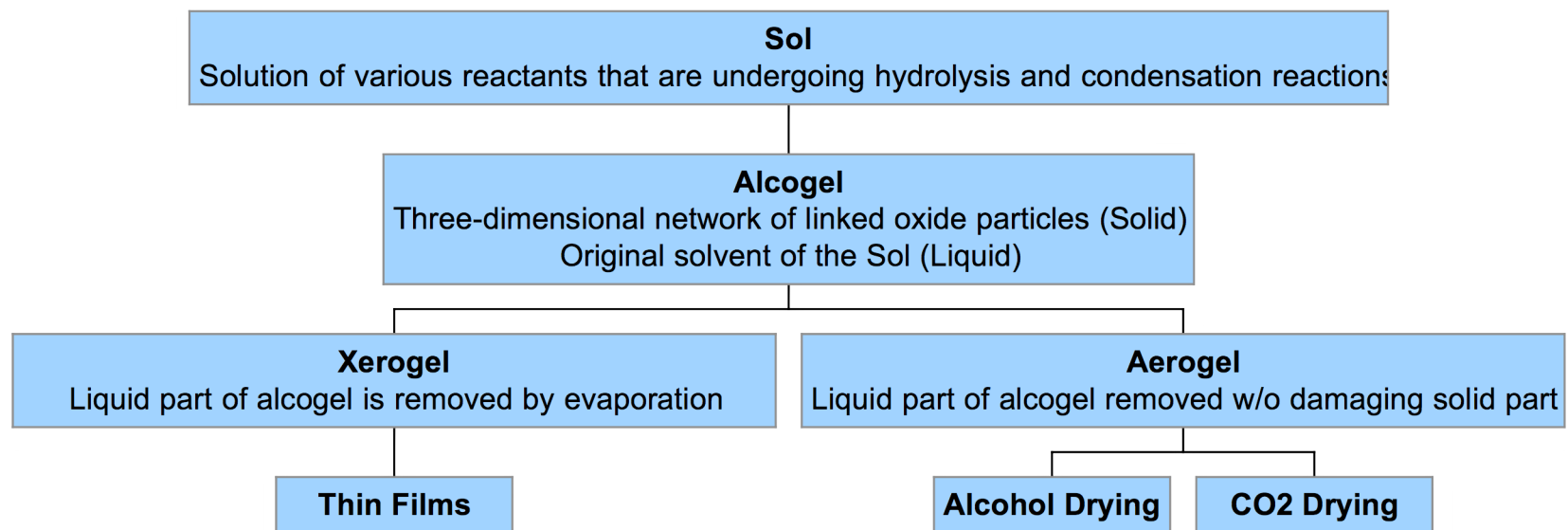


Figure 1.5 – Illustration of the sol-gel terminology



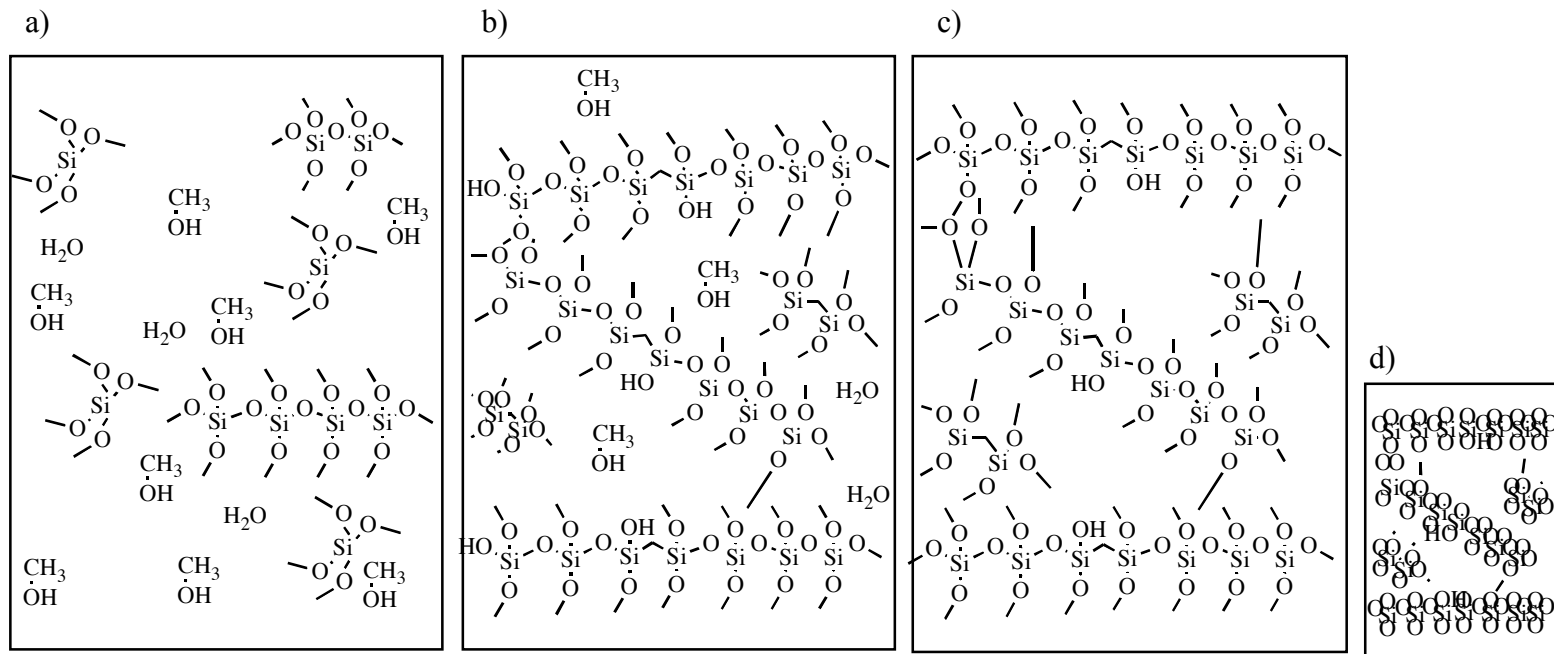


Figure 1.6 - Pictorial representation of chemical reaction of a) liquid sol, b) alcogel, c) aerogel, d) xerogel

“Aerogel” – (Figure 1.6c) If the solvent from the alcogel is removed, by methods described later in Chapters 3 and 4, without a collapse of the network, an aerogel remains.

“Xerogel”- (Figure 1.6d) A xerogel is formed from letting the solvents evaporate from the alcogel. The porous network collapses and depending on concentration of silica network to solvent, the xerogel shrinks considerably and still maintains the general dimensions of the container from which the alcogel was formed.

Each of these materials is discussed at length in the subsequent chapters.

### **1.3 Review of Literature**

As quantum dot research becomes more prevalent, interest grows in experiments to embed semiconducting nanocrystals in various materials. This section will discuss the recent and relevant research in the topics covered by this thesis. Consequently, this review will consist of two main topics. The first will be a review of recent research that has been completed or is ongoing on materials studies of quantum dots in sol-gel processed glass. I will encompass the different ways that various groups have achieved their goals, challenges that they encountered, and to what purpose they feel their material can serve. This section will also include the few papers that have been published on aerogels containing quantum dots.

The Mulvaney group out of the University of Melbourne has published synthesis work that creates photo-stable quantum dot glasses using the sol-gel process and highlighted stability of quantum dots during gelation as a main challenge [9]. Their procedure takes CdSe quantum dots where the surface has been core-shelled with ZnS and capped with trioctylphosphine (TOP) and trioctylphosphine oxide (TOPO). To create the sol-gel, the group adds TMOS and octylamine as a catalyst. The materials produced are relatively stable for months after preparation and their data shows no significant change in quantum dot size.

Similarly, work recently published out of the University of Arizona at Tempe also uses TMOS in an alcohol solvent to create silica monoliths [10]. Wang *et al.* produced silica disks and embedded differing sized quantum dots in each. The ligand used for quantum dot capping in this experiment was 3-mercaptopropyltrimethoxysilane (MPS.) The thiol group has a large binding affinity for the surface of the quantum dot while at the other end of the molecule; the silica groups can react with the sol-gel reaction and create tighter connections into forming glass.

Previous to this research, Liz-Marzan *et al.* produced quantum dot glasses containing CdS [11,12]. Unlike research using TMOS as the primary silica source, their work uses the cross hydrolysis and condensation of the alkylsilane capping ligand to create a gel. Mainly, they use 3-aminopropyltrimethoxysilane (APS) to cap the quantum dots as well as excess APS to cause the gel reaction to finally form a monolith. As Mulvaney discusses in his research, this method alters the emission of the quantum dot so the photoluminescence is predominated by trap emission.

Also a group from the Photonics Research Institute in Japan uses the cross-condensation of capping ligand is [13,14]. The primary quantum dot material they use for this research is CdTe and they spin coat the viscous gel onto glass slides. The most recent paper discusses the photodegradation of the quantum dots used and concluded that it is either linked to the oxidation from the first electronically excited state or a surface change related to surfactant reactions.

Recent research that just begins to delve into the subject of taking quantum dot semiconductors in silica aerogels was published in January of 2005 [15]. Brock's group from Wayne State University created the aerogel material using gelation through controlled surface-group loss. This procedure does not create a 'true' aerogel comprised mainly of silicon-oxygen bonds and therefore is described as 'aerogel-like.'

## **1.4 Summary of Chapters**

The following is a brief description of subsequent chapters. Chapter 2, Xerogel Synthesis, will detail the procedures to obtain reproducible xerogel samples with embedded quantum dots. It includes references to quantum dot synthesis, ligand exchange, TMOS solution preparation, gel aging and drying, and analysis of samples. Chapter 3, Aerogel Synthesis, takes the alcogel samples and describes aerogel sample preparation and analysis. Chapter 4, Critical Point Drying Procedure, specifically details the workings and procedure for the critical point dryer that is used in aerogel formation. Chapter 5, Primitive Sensor Experiments, delves into the background research for sensor requirements and looks at the response of CdSe quantum dots as sensors for explosives. Finally, this thesis will finish with Chapter 6, Conclusions and Unanswered Questions.

## CHAPTER 2

### XEROGEL SYNTHESIS

#### 2.1 Chemical Preparation of Quantum Dot Sol

Silica sol-gel synthesis has been extensively studied and this chapter is by no means meant to encompass all areas of this research. If you are interested in the various intricacies of sol-gels there are references that can start you on your way [16].

The formation of a wet gel is obtained by adding silica alkoxide precursors together with water in an alcohol solvent. Common silica alkoxide precursors include tetramethylorthosilicate (TMOS) and tetraethylorthosilicate (TEOS). Sol-gel chemistry begins as soon as the precursors are added together and can take up to seven days for the silica network to branch across the three-dimensional space of the container it occupies, or its ‘gel point.’ Once the gel-point is reached it can take additional days for the hydrolysis and condensation to completely form the silica-oxygen network. The ‘aging’ of the wet silica sol-gel occurs while the gel is soaked in an alcohol/water mix with a concentration that is similar to the original reaction. As stated in the previous chapter, the general balanced formula for the silica sol-gel reaction is referred to in Figure 2.1.



Figure 2.1 – General sol-gel reaction

While only two moles of water is required per one mole of silica alkoxy molecule, generally more water (up to 30 times more) is used to improve the optical clarity and stability of

the reaction. The sol-gel reaction is kinetically slow and therefore is normally catalyzed by an acid or base. The acid catalyzed reaction works by speeding up the condensation step while the base catalyzed reaction works by speeding up the hydrolysis step.

### **2.1.1 Sample Sol-Gel Procedure**

Measure 15.15 mL of HPLC-grade methanol into a 50 mL container (beaker A). In a hood, slowly add 15.15 mL of TMOS to beaker A and stir gently. For consistent results, use freshly distilled TMOS that has pre-hydrolyzed silica removed or flush reagent bottle with inert gas after each use to remove atmospheric water. TMOS container can be backfilled with a dry, inert gas to prevent hydrolysis and condensation. In a separate container (beaker B) mix 14.31 mL of HPLC-grade methanol and 5.57 mL of distilled water. While stirring beaker A, slowly add mixed contents of beaker B. At this moment, the hydrolysis and condensation reactions have begun. The sol-gel solution can be dispensed into desired containers to allow for alcogel formation. Take note of the approximate amount of ligand containing silica, if the volume is appreciable, then the amount will need to be added to the molar ratio of silica. Solution will continue to be liquid for around seven days. Any acid, base, or amine solutions added to condensing gel will act as a catalyst for the reaction and decrease time of gel formation. Even a small amount of amine will reduce gel formation time to a few minutes.

### **2.1.2 Chemical Preparation of Synthesized Quantum Dots**

The quantum dot samples that were used were all prepared via microwave synthesis as published [17]. The quantum dot samples were cleaned and capped with a ZnS shell as described by the SILAR method [18]. The emission and excitation spectra of the 2.5 and 6 nm CdSe/ZnS and the InP used in this thesis are found in Figure 2.2.

### **2.1.3 Ligand Selection**

During my preliminary studies, I experimented with various silicon-containing or water-soluble ligands. Description of attempted ligands and their various problems can be seen in Table 2.1. The most successful ligand was 3-aminopropyltriethoxysilane (APeS). Although the thiol version of this ligand has also been successful, the amine catalyzed the reaction to produce more robust gels for supercritical drying. This is typically seen in silica sol-gel synthesis: base-catalysis is used to improve aerogel structure integrity.

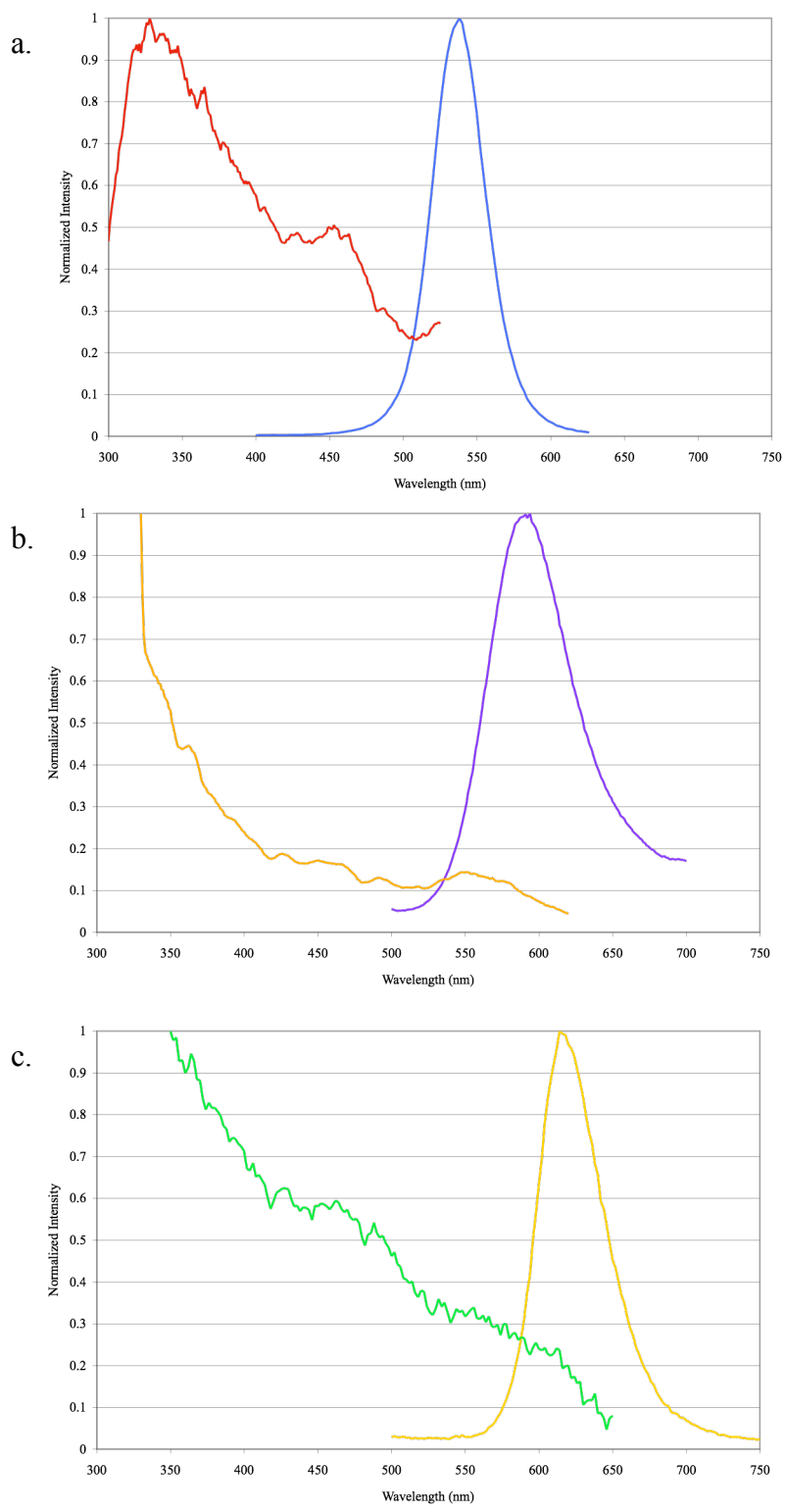
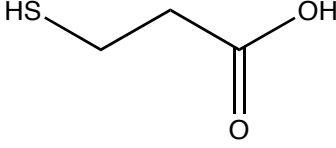
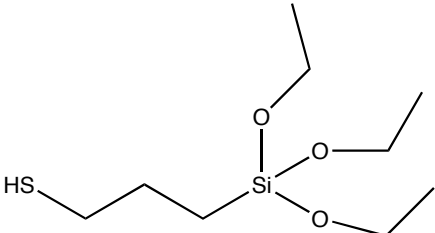
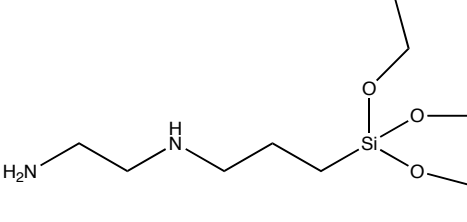
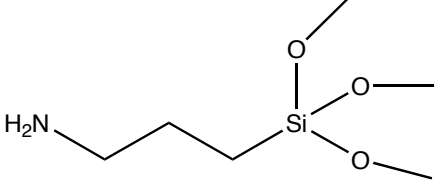
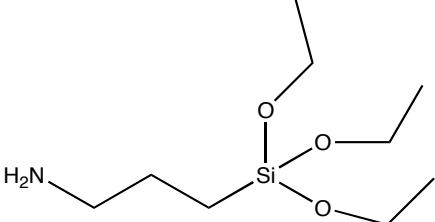


Figure 2.2: Excitation and emission of a) 2.5nm CdSe/ZnS b) InP/ZnS and c) 6 nm CdSe/ZnS parent dots used for xerogels and aerogels.

Table 2.1 – Table of Quantum Dots Ligand Variations Attempted for Sol-Gel

Ligand Chemical Name (abrv) [CAS]	Structure	Figure of Merit, PL Intensity & Stability
Mercaptopropionic Acid (MPA) [79-42-5]		Created water-soluble dots that created optically transparent glasses. Stability of luminescence for days
3-Mercaptopropyl triethoxysilane (MPS) [4420-74-0]		Optically transparent glasses, very stable xerogels, soft aerogel stable for days
Aminoethylaminopropyl triethoxysilane (AEAPES) [1760-24-3]		Minimally stable luminescence
Aminopropyltrimethoxysilane (APS) [13822-56-5]		No stable luminescence
3-Aminopropyltriethoxysilane (APeS) [919-30-2]		Most stable of all ligands, rigid aerogels, luminescence stable

The first ligand I tried to make the quantum dots water-soluble was APS. APS is frequently referenced in the literature to make silica glasses with quantum dots. This method caps the quantum dots in excess APS. After adding a molar ratio of APS:MeOH equal to 1:30. The APS cross-condenses to first form a viscous solution and then a glass. Although I attempted to reproduce this method, I could never get the quality of glass that I get through the TMOS method. APS cross-condensed glass was optically transparent but very dense and did not condense like TMOS glass. Therefore APS glass was very difficult to remove from the container from which it was formed without damaging the sample.

#### **2.1.4 Ligand Exchange Procedure**

The first step to ligand exchange from HDA to APeS was to dissolve 100 to 300 mg of sample in 0.25 mL of chloroform and precipitate the dots with 5mL MeOH. Centrifuge sample and remove supernant. Repeat cleaning up to three times for greatest quantity of HDA removal. Dry pellet under vacuum.

APeS was then added to the test tube in the smallest amount to dissolve quantum dot, approximately 0.5 mL. Since the ligand is already methanol-soluble, it is difficult to precipitate the re-capped dots out of the solution. I got around this by adding the smallest amount necessary. If the dot does not go into solution immediately or after sonicating, gently heat in a warm water bath set to 60-80°C for 20 minutes. I then would add an equal amount of methanol to the test tube and quickly centrifuge out any dots not suspended in solution. Normally after centrifuging, the supernant was optically transparent and filled with quantum dots. Generally, anywhere from 50 to 100% of dots remained in supernant. I would then check luminescence under a hand lamp before adding to pre-poured TMOS molds.

#### **2.1.5 Creating a Gel**

With TMOS solution and re-capped dots prepared, a clean and dry container was selected to create within it a gel. Care was taken to choose the right container; a xerogel shrinks considerably depending on concentration of TMOS added. The gel will shatter and shard if the container is too large or the condensation too rapid. If possible, multiple gels were created to increase probability of the best product. A measured amount of TMOS solution was placed into the containers followed by the addition of the APeS solution. The mixed gel was gently but rapidly stirred and care was taken not to introduce bubbles or eddy currents to the forming gel. See Figures 2.3-2.4 for illustrations of gel formation. For these photos, 0.5 mL of APeS/MeOH



solution was added to each Petri dish and contained approximately 1 mg of 2.5 nm CdSe/ZnS. After the gel is allowed to shrink, the concentration of the dots increase and they are easier to see.

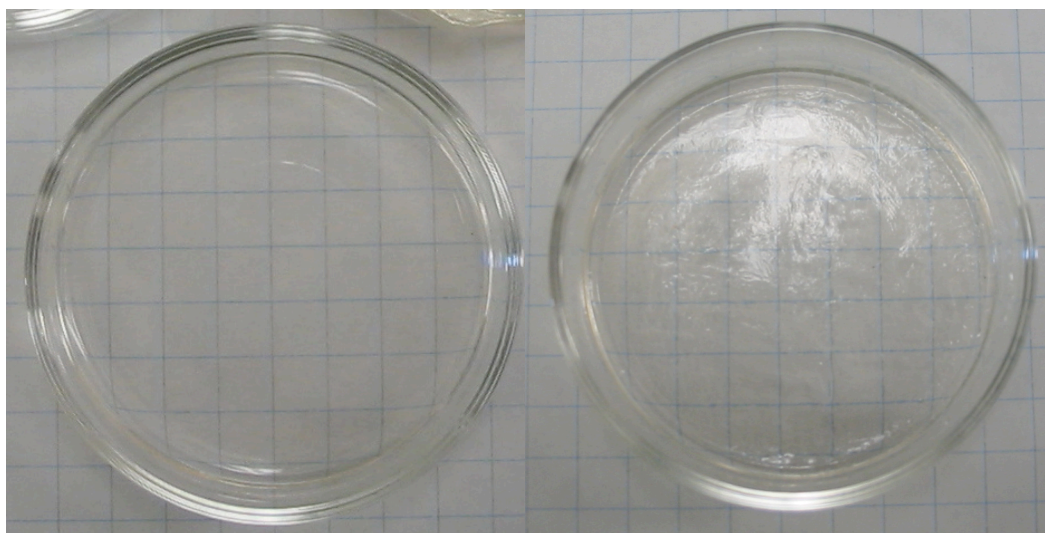


Figure 2.3 – Picture of liquid gel after quantum dot solution has been added (left) and after gel has formed (right).

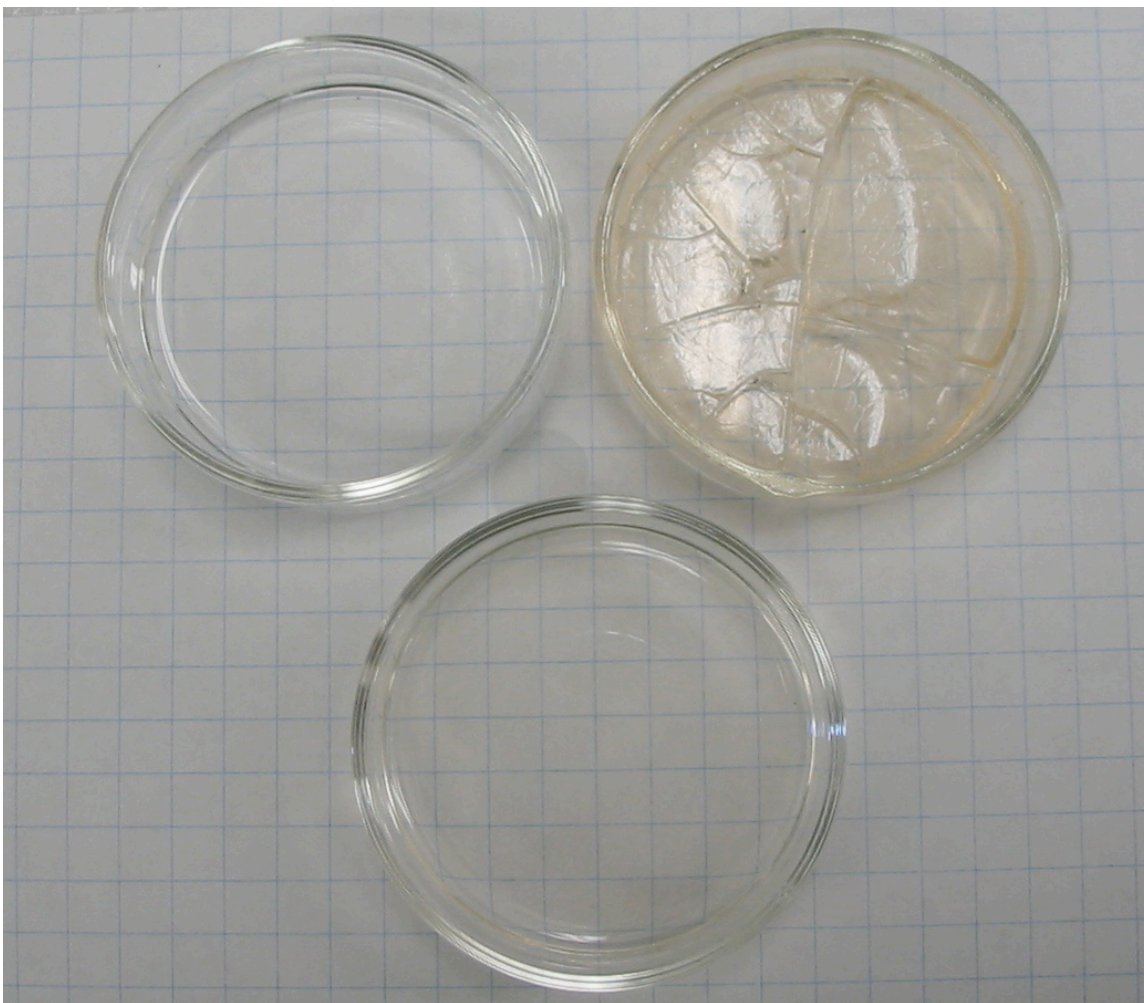


Figure 2.4 – Three dishes showing progressing reaction. First (top-left) is TMOS solution only. The second (lower) is liquid sol-gel with quantum dot added before condensation. Finally, the third (top-right) shows what happens when the reaction is too vigorous and gel quickly cracks.

### 2.1.6 Gel Instabilities

Figure 2.5 illustrates one of the challenges of the xerogel preparation using embedded quantum dots. Under unknown atmospheric changes of humidity and ambient temperature one disk of a set of xerogel monoliths has gone cloudy. One idea of the reason for this clear to cloudy transition is the excess of hexadecylamine (HDA) left in the TMOS gel. The quantum dot is initially stabilized by HDA to minimize surface oxidation and is not fully removed by the ligand exchange procedure. We have seen that these changes occur during a multitude of non-reproducible stresses, such as laser excitation of the disk, changes in temperature or humidity, or physical pressure. We find that we can force the gel to become clear again by gently heating, placing in desiccators, or waiting for the reverse change to occur again. The effect, while intriguing, is not well understood at this time.

To help understand this peculiar transition, we took a portion of an InP xerogel and calcined it to 500°C over the course of a week. The sample had less than a 5% weight loss after it was calcined and all the solvent, quantum dot, and organic ligand are burnt out of the gel. This sample was crushed and surface area and porosity information obtained through gas physisorption (BET analysis) using a Micromeritics® ASAP 2020. The surface area calculation was 448 m<sup>2</sup>/g, with a pore size of 3.16 nm. The same uncalcined sample had a surface area of 433 m<sup>2</sup>/g with a pore size of 3.8 nm. The type 2 linear isotherm plots of both samples can be found in Figure 2.6. Although I would expect a smaller pore size for the uncalcined xerogel, the pores may have collapsed while the quantum dot was burned out. More work can be done to understand the apparent liquid crystal condensation and reversal of these xerogels.

In addition to the cloudy/clear transitions, the creation of a gel is not always reproducible. What seem to be identical gels created at different times can greatly vary in resulting luminescence once allowed to dry. Since the process from gel mixing to a finished result can take weeks, any slight inconsistencies in this timeline can change outcome. Also, when a gel is formed, it appears to go through ‘cycles’ of bright and dim luminescence. Quite often have I deemed a sample to be ‘dead’ only to find it glowing again the following week.

I most often worked with the 2.5 nm CdSe/ZnS dot and noticed that the gels that ended up yellow in color were often very bright emitters while the same concentration gels that remained orange in color are weakly luminescent. I could not find any difference in either gel in the way they were created.



Figure 2.5 - Two CdSe/ZnS Xerogel monoliths prepared with identical quantum dot concentration and conditions. Gel on left has gone spontaneously cloudy while gel on right is clear.

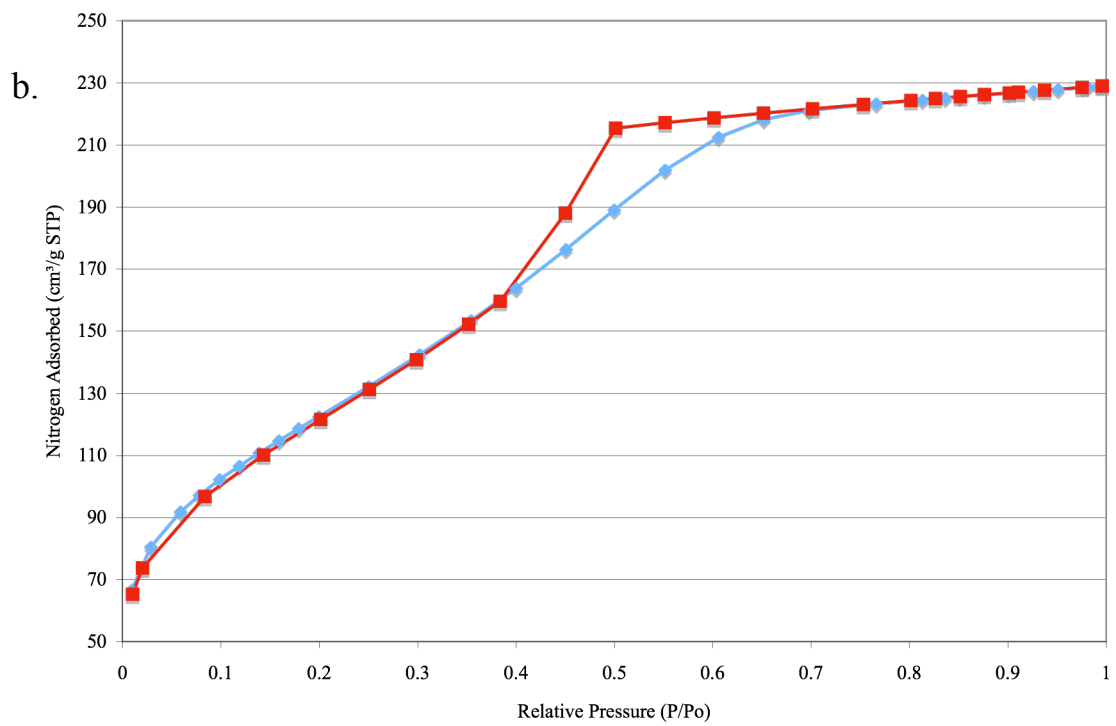
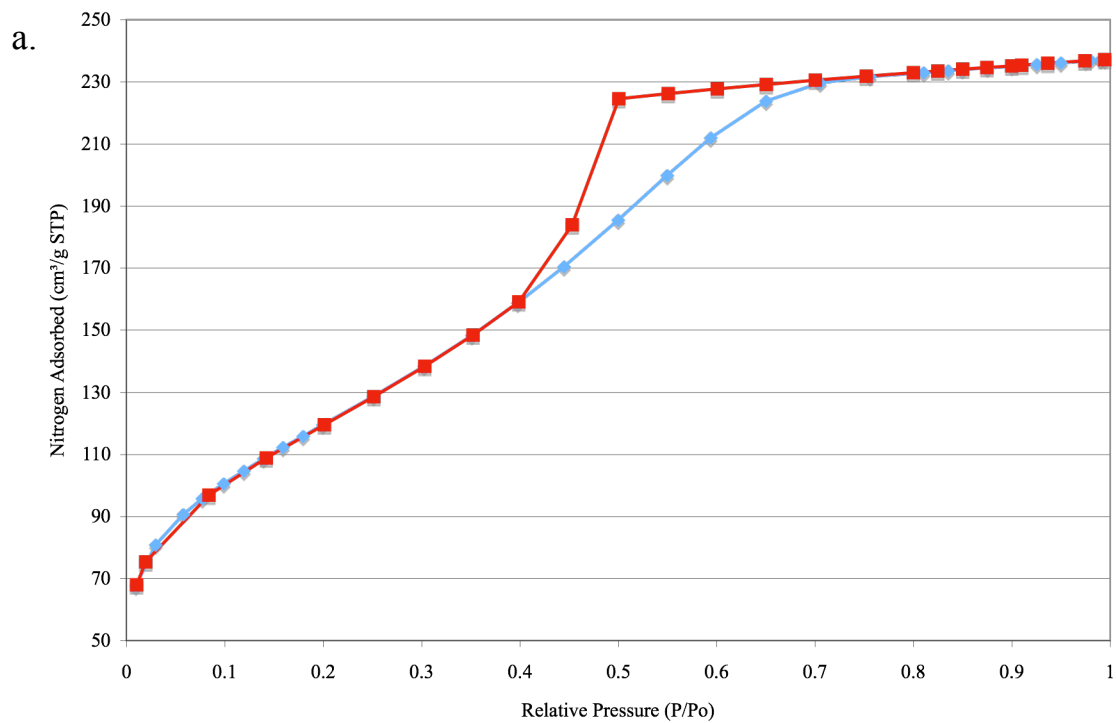


Figure 2.6 - Isotherm plots for nitrogen physisorption of a) calcined and b) uncalcined InP xerogels.

### 2.1.7 Heat-treating gels to remove solvent

After a gel is formed, aged, and reduced to size where it no longer has the chance to crack or shard, the gel can be gently heated to 70°C to help remove remaining solvent. Normally, a xerogel is placed through the calcining process. This process very gradually exposes the gel to warmer temperatures under an inert or selected gas. While I did this on a few samples, the extreme temperatures that this process takes the xerogels to would disable the desired properties of the quantum dot. Normally, after a gel had been left to sit for several weeks, it was placed in an oven in air and gently taken up to 70 to 100°C. I would ramp up the temperature 5°C per hour. For future studies, I recommend this process be completed under an inert environment to reduce exposure to oxygen.

Thermal analysis DSC/TGA of a xerogel was taken on a TA Instruments SDT 2960. In Figure 2.7 are results from a DSC/TGA (Differential Scanning Calorimeter – Thermogravimetric Analysis.) A small piece of xerogel was first run under oxygen as flow gas at 100 mL/min and then a new sample was used for the nitrogen gas at the same flow volume. Figure 2.8 shows the blank xerogel and a CdSe quantum dot in the DSC/TGA for comparison purposes. The CdSe quantum dot shows weight loss at an earlier temperature than the xerogels. This is perhaps because it is less exposed after the embedding or the ligands helps stabilize it differently.

The DSC-TGA data for both quantum dot embedded xerogels show that a significant portion of the solvent left in the xerogel is baked off by around 175°C and when you raise the temperature above 300°C the ligand is removed and the surface of the quantum dot is oxidized. This data supports the experimental method of baking xerogels up to 70°C to 100°C to remove most of the solvent. This data also shows how under oxygen environment the surface of the dot will oxidize at high temperatures. An interesting future experiment would be to synthesize the xerogels under a nitrogen environment to test for improvement in luminescence.

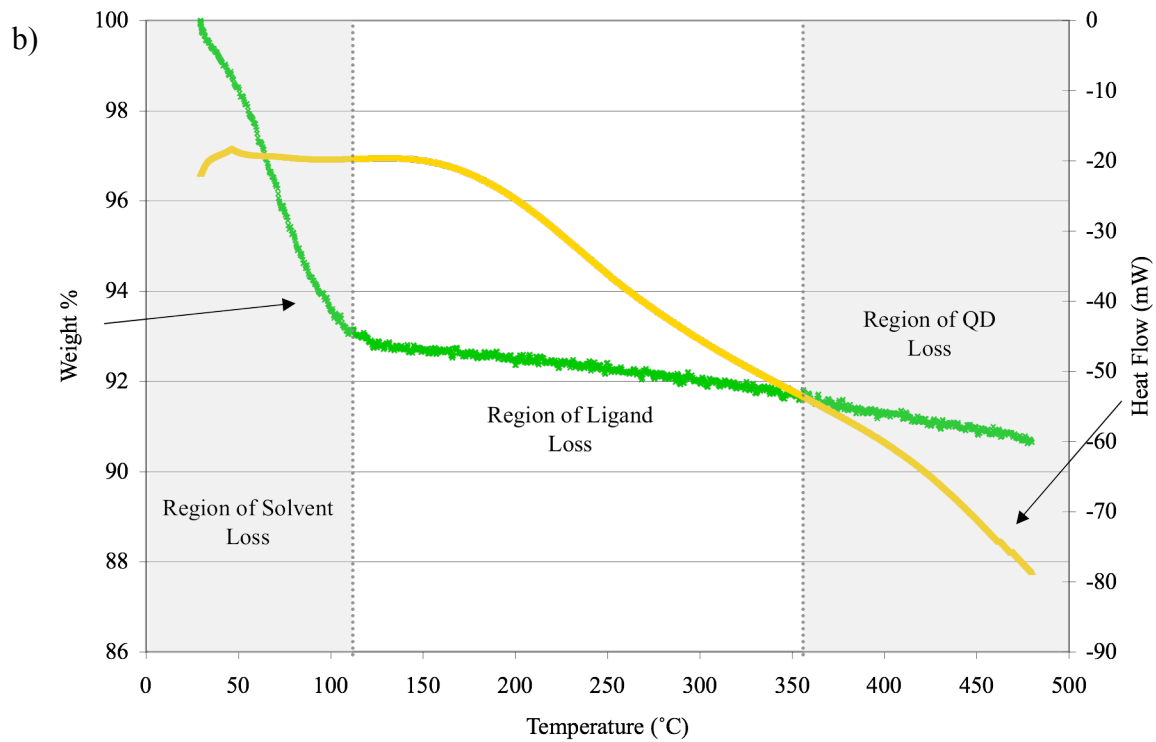
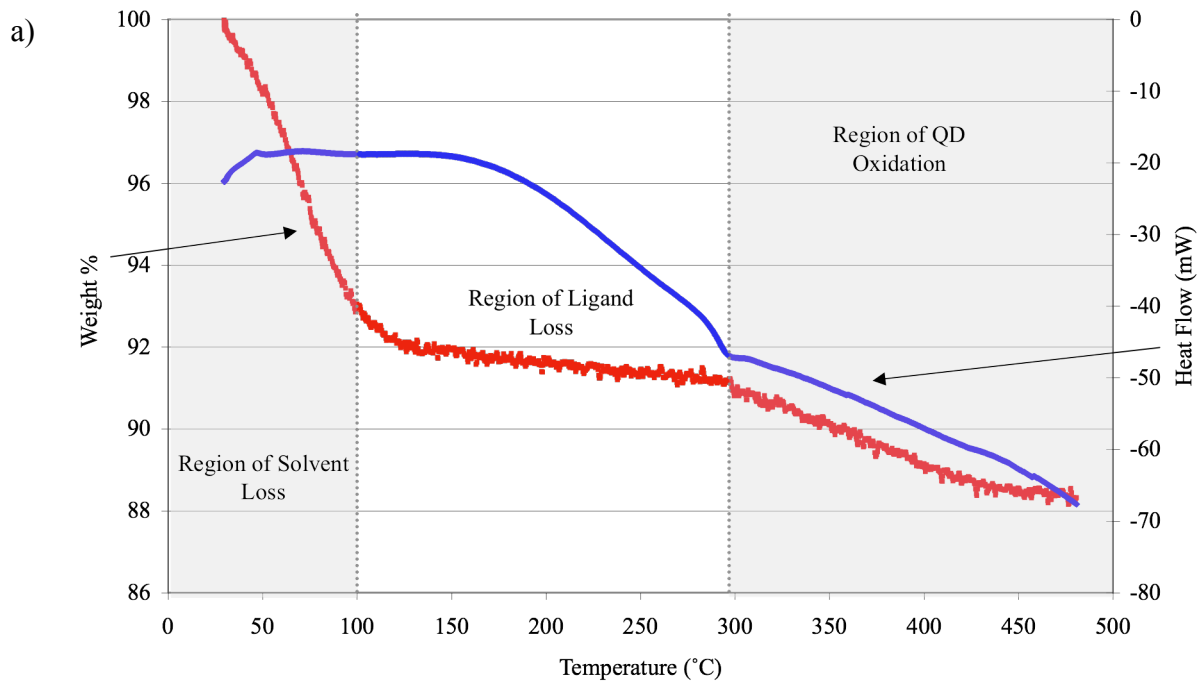


Figure 2.7 – DSC-TGA data for uncalcined CdSe xerogel under a) oxygen and b) nitrogen gas flow.

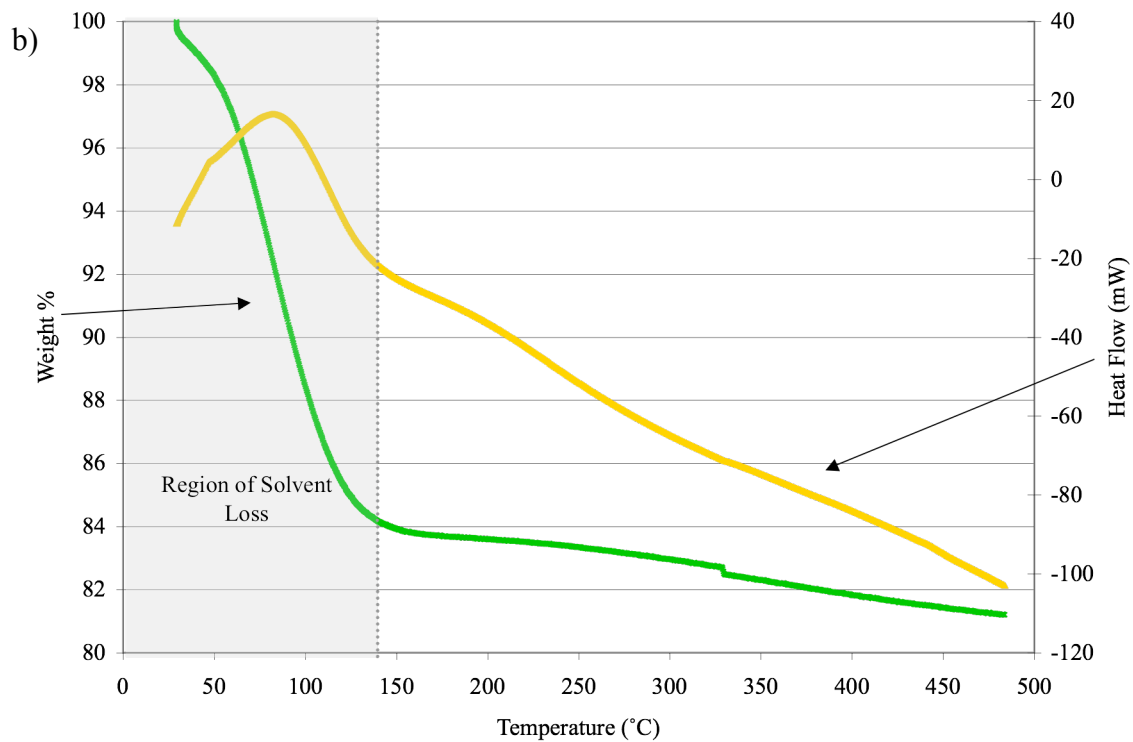
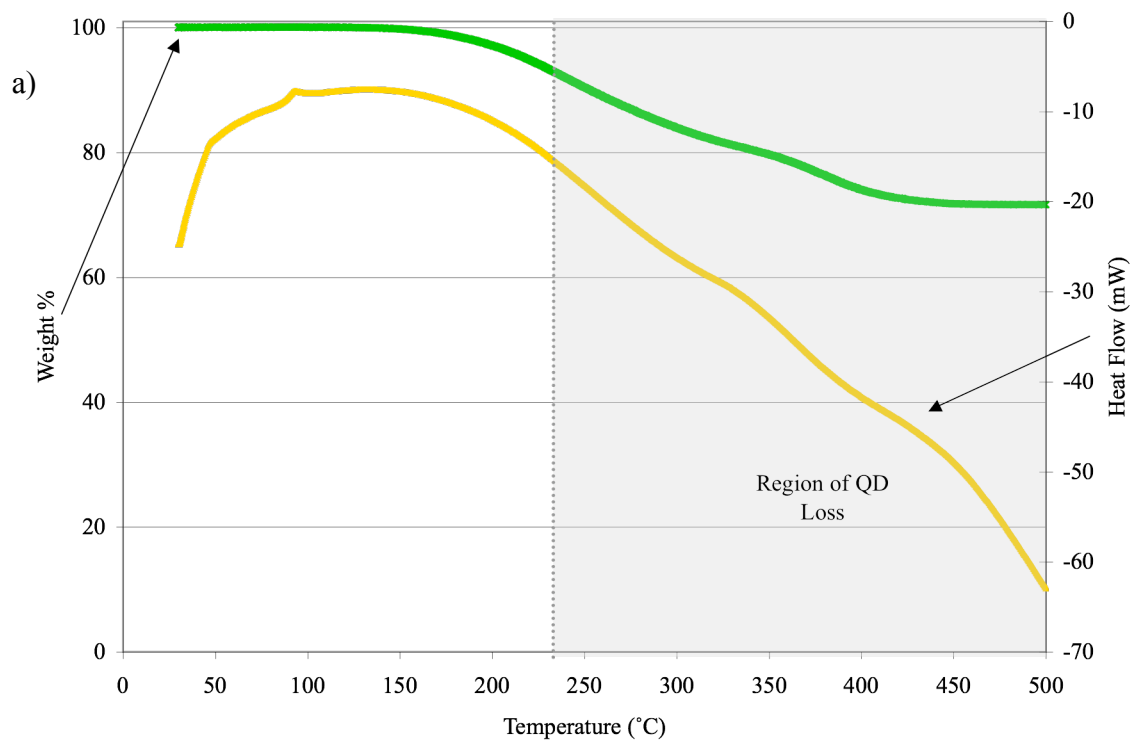


Figure 2.8 – DSC-TGA data for a) pure CdSe quantum dot and b) blank xerogel both under nitrogen.



## 2.2 Experimental Analysis of Xerogels

### 2.2.1 Photoluminescent Results

The photoluminescence data was taken on a SPEX Fluorolog 1680 with 0.22 m double spectrometers. Data was taken in the ‘front-face’ mode because the optical clarity of samples varied and most data was taken with 2.5 mm slits. Weakly luminescent samples were taken with 5.0mm slits and can be distinguished from the large tin impurity peak at 420nm. Figure 2.9 shows how bright the luminescence from the dried gels can be. The luminescence on this particular sample, which was unfortunately broken while heating, is visible under room light with a UV hand lamp. Figure 2.10 shows luminescence of a heat-treated 2.5 nm CdSe/ZnS xerogel and the parent dot solution. The peak shows a 10 nm blue shift, most likely due to oxidation of the passivating ZnS surface during condensation of the gel. The peak also shows the tin impurities present in the TMOS solution that add a peak at 420 nm [19]. A further study of the stability of dots in the sol-gel matrix could be completed with various capping thicknesses of the quantum dot. This may solve the ‘etching’ of the surface from the condensation process. Figure 2.11 depicts the graph of InP/ZnS xerogel luminescence. The signal is very dim and therefore the tin impurity peak at 402 nm is clearly visible

I also looked into the change in luminescence over the formation time of the gel, from before addition of quantum dot to 24 hours after gel formation. The data shows that there is a significant change in luminescence as the gel forms as seen in Figure 2.12. The luminescence drastically decreases and then recovers 24 hours later. This could be due to the heat generated during the gelation process or the rapid chemistry that is occurring. The gel was only studied to 24 hours after formation because after that time, the gel begins to shrink and its dimensions change in a non-homogeneous fashion.

### 2.2.2 Acetonitrile Brightening

An interesting result occurred early in the quest to find a stable ligand for gel formation. I was using different wash solvents to replace excess methanol after the gel had formed. This process is critical to solvent exchange in supercritical drying, described in subsequent chapters. While using HPLC-grade acetonitrile as a wash solvent and MPA as the ligand, the gels dramatically increased in photoluminescence and remained brightened for weeks. Eventually the luminescence of the dots ceased which caused us to move on to the other ligands. This concept

of using a solvent other than MeOH or EtOH could add another possibility for fine-tuning the manufacturing of high quality samples.

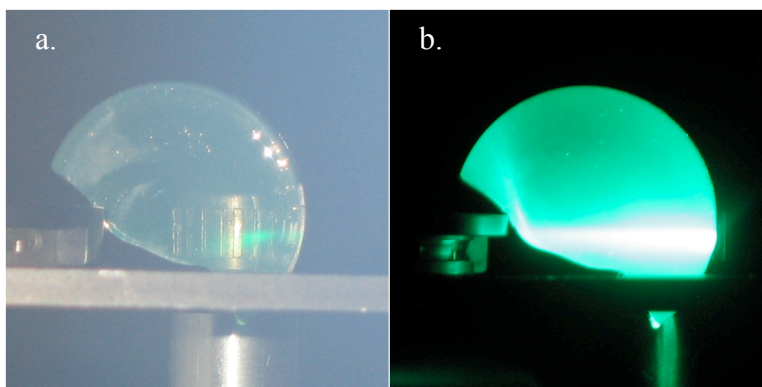


Figure 2.9 – Photo of approximately 3 mg of 2.5 nm CdSe/ZnS 5 cm diameter xerogel disk excited with 1 mW 488 nm laser and viewed through a 488 nm filter in a) room light and b) dark.

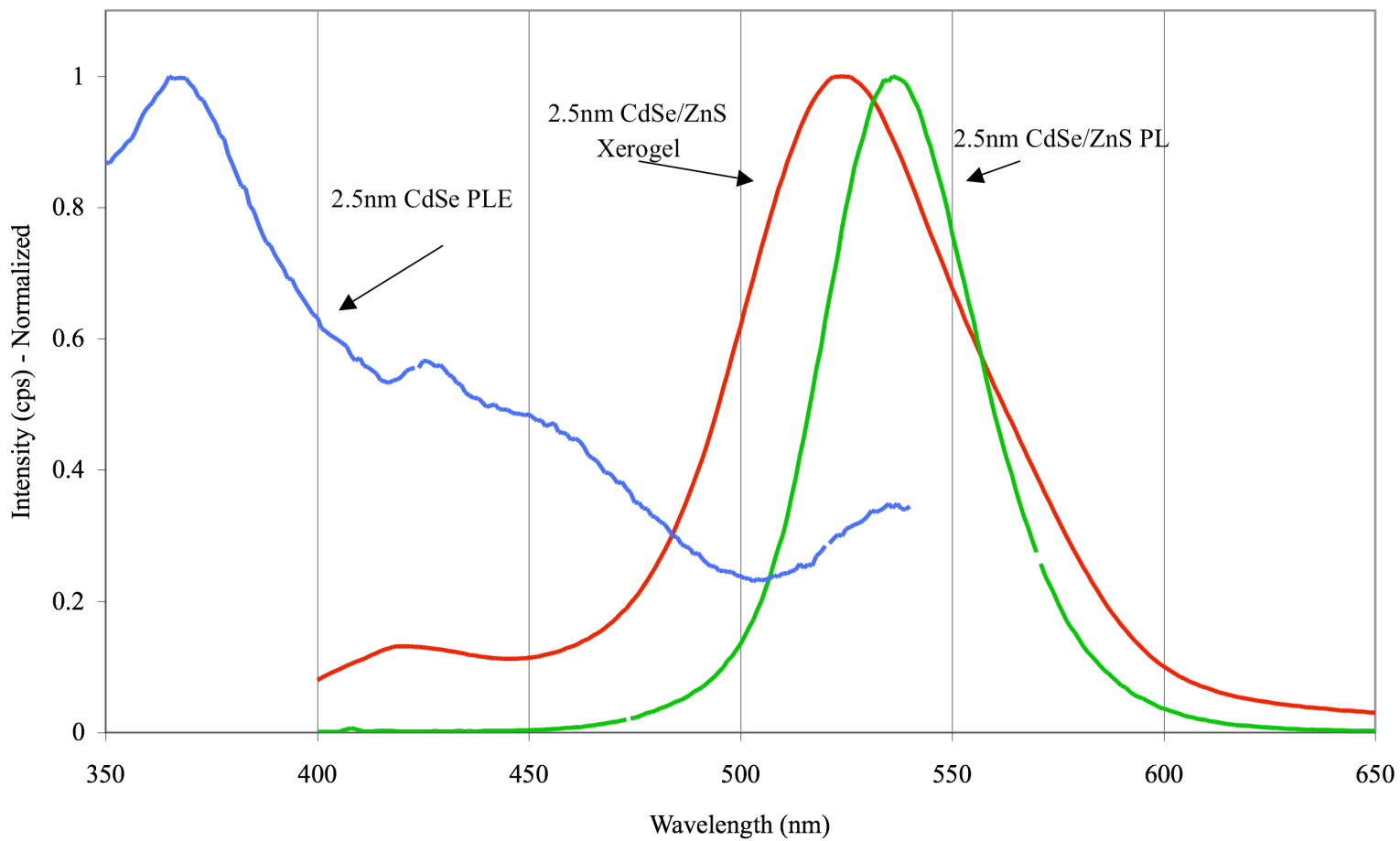


Figure 2.10 – Graph of normalized photoluminescence intensity of dried CdSe/ZnS xerogel and parent dot solution.

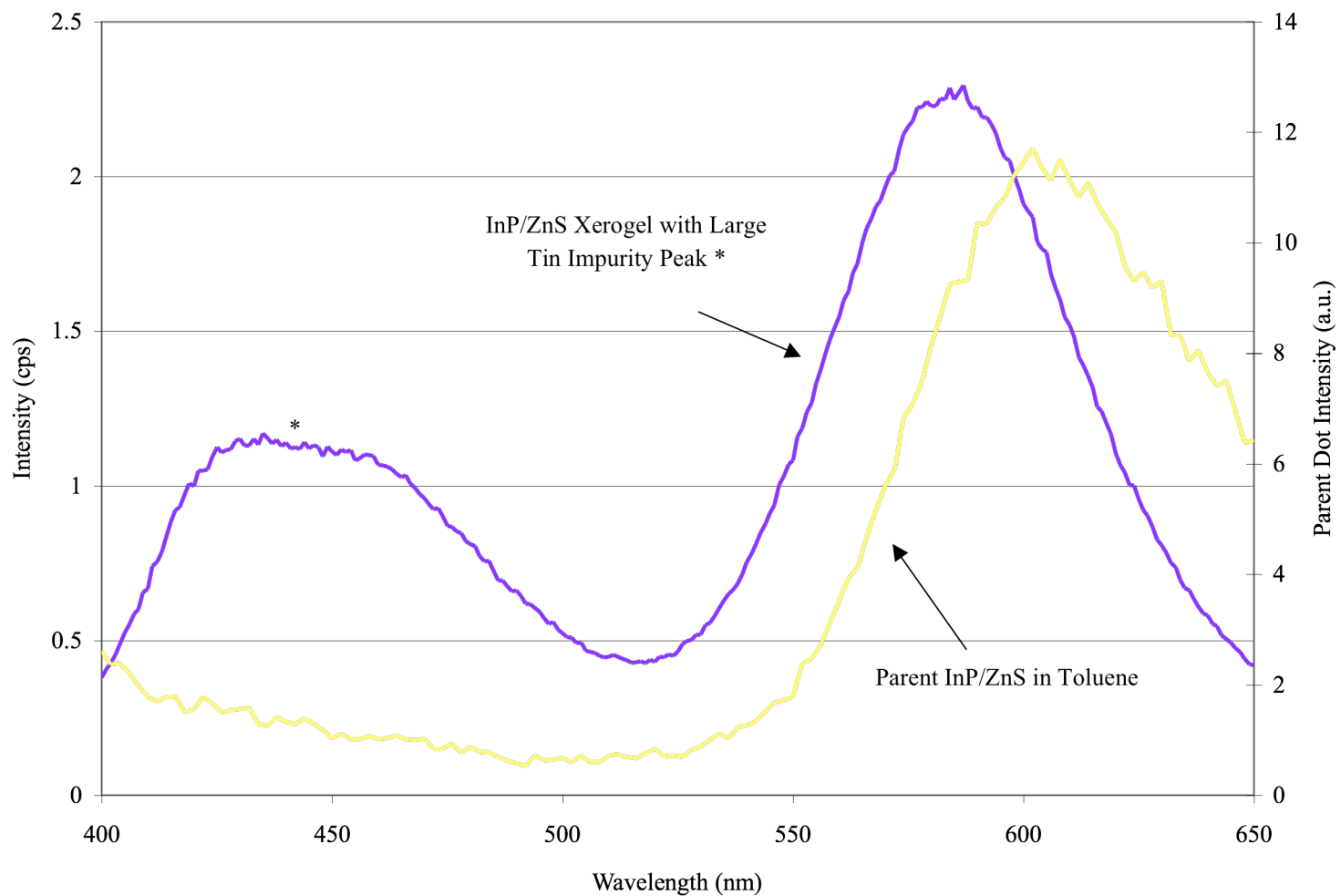


Figure 2.11 – Photoluminescence of InP/ZnS xerogel and parent dot solution. Luminescence is very weak and impurity peak at 420 that originates from tin impurities in TMOS is evident.

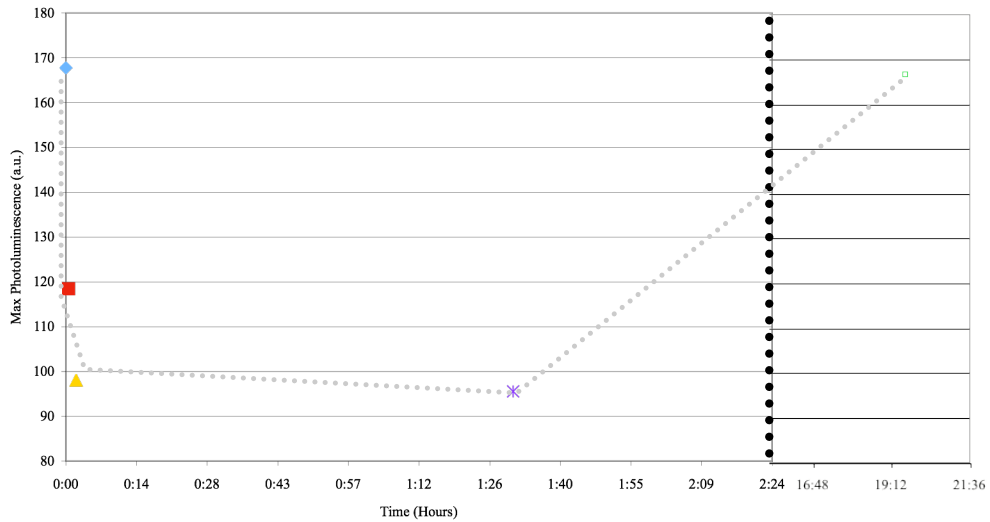
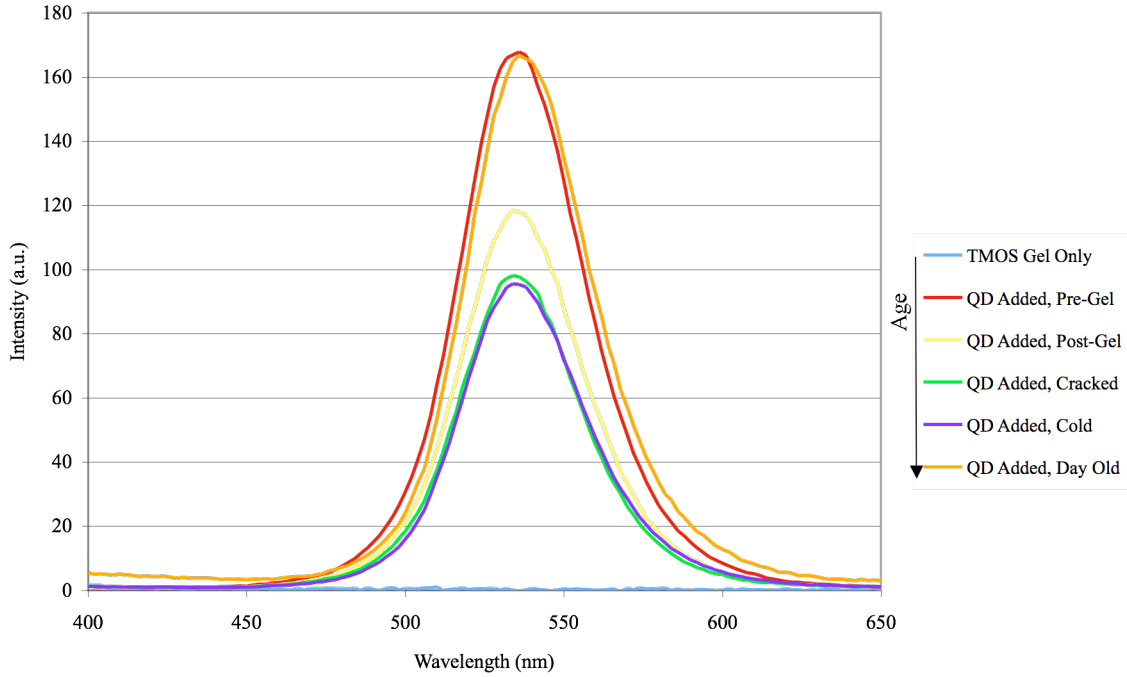


Figure 2.12 – Tracking of 2.5 nm CdSe/ZnS xerogel photoluminescence tracked over 24 hours as a) intensity b) maximum intensity tracked through time.

## CHAPTER 3

### AEROGEL SYNTHESIS

#### 3.1 Aerogel Introduction

##### 3.1.1 Background

Semiconductor quantum dots, of which CdSe is prototypical, have garnered considerable attention for optical application because of their high luminescent intensity, photostability and chromatic tunability [20]. Integration of quantum dot luminophores into optical components often requires their homogeneous incorporation into a transparent matrix. Approaches to accomplishing this have included dispersion in organic polymers, and their in-situ nucleation in molten glass [21-25].

Sol-gel processing, an obvious approach to sequestering QD in an oxide matrix, has been successfully used for thin film formation, however, due to inherent incompatibilities between the surface chemistry of the QD and the sol-gel process itself, large monolithic silica structures have been more difficult to produce [26]. Recently, studies outlining the successful dispersion of CdSe/ZnS core/shell QDs in a monolithic silica sol-gel material have appeared. Initial studies by Selvin *et. al.*, reported the use of alkylamine with CdSe/ZnS to perform the dual role of surface passivation and catalysis of the sol-gel reaction [27]. Luminescence of the QD was preserved through gelation and for several months during aging but ultimately emissive intensity was lost. More recently, Wang *et. al.* have reported the fabrication of monolithic silica xerogels containing CdSe/ZnS QD of varying sizes that retained their emissive properties. This synthetic approach utilized a 3-mercaptopropyltrimethoxysilane capping ligand that cross-links into the silica matrix thereby stabilizing the dots in the matrix [28].

### 3.1.2 Applications

Among the most promising application of quantum dots is in the area of chemical sensing where the surface chemistry of the QD can be tailored to recognize specific analytes, which, in turn, either quench or brighten the luminescence. For sensing applications, a high surface area that affords rapid mass transport to the surface of the QD is desirable. As such, ultra low-density silica aerogel materials are an excellent medium for sensor applications as they can be nearly transparent and have extremely large surface areas. We report here the first successful fabrication of stable low-density silica aerogels with dispersed CdSe/ZnS quantum dots.

### 3.2 Synthesis and Analysis

Alcogels containing CdSe/ZnS quantum dots were made from tetramethylorthosilicate (TMOS) and water in methanol cosolvent (3:1:6 by vol). The ZnS capped CdSe QDs of 6 and 2.5 nm dimension were made by published procedures and were capped with 3-aminopropyltriethoxysilane (APeS) [29, 30]. This capping ligand provided surface passivation and couples covalently with the silica matrix to secure the quantum dot during the supercritical extraction process. In addition, the excess ligand, which is present in the sol-gel solution, acts as a catalyst. Bases catalyze the condensation process in sol-gel chemistry thereby making hydrolysis rate determining so that most hydroxyls produced immediately condense through either alcohol or water forming processes [31]. This yields a highly branched silica network, which is preferable for aerogel formation due to its rigidity. In a typical aerogel preparation, the desired quantities of APeS treated QD were added to the aqueous TMOS solution with rapid stirring. Gelation times ranged from 30 second to 5 minutes depending on the amount of APeS treated QD added. The gelation was carried out in a mesh mold, which was placed in a sealed container. After gelation the alcogel was submerged in a methanol solution and allowed to age for a period of 24 hours. After aging, the gel was washed successively with dry methanol or dry acetone. This washing process was repeated every four hours for two days to fully remove water and unreacted APeS from the gel. The basket and final methanol wash was then placed in a supercritical extractor, cooled to 7°C, and flushed with liquid CO<sub>2</sub> to remove the methanol and replace it with liquid CO<sub>2</sub>.

The liquid CO<sub>2</sub> is subsequently flushed and replaced every three hours to remove all the organic solvent from the gel. While the number of CO<sub>2</sub> exchange cycles depends on the size of the aerogel, for the 1'1'5 cm monolithic aerogel that were typically produced, 7 cycles were required to complete the solvent exchange. After washing was completed the liquid CO<sub>2</sub> was taken to 35 °C and the CO<sub>2</sub> was taken above its critical point with an internal pressure of ~1100 psi (it was not allowed to exceed 1200 psi). The extractor was then vented slowly over a period of 1 hour.



Figure 3.1 - Silica aerogel containing 2.5 nm CdSe/ZnS quantum dots.

This QD embedded aerogels produced with APeS as a catalyst are of very high quality with good transparency (Figure 3.1). The measured density is 300 mg/cm<sup>3</sup> and the surface area, from



gas physisorption (BET analysis), is 789.7 m<sup>2</sup>/g. The UV-Vis spectrum (Figure 3.2), collected as a transmission spectrum through a 5 mm thick aerogel containing the 2.5 nm QDs, has a transmittance of ~68% in the visible, which is typical of good quality silica aerogels in this density range (though not as transparent as extremely very low density aerogels) [32]. The extinction mechanism is dominated by Rayleigh scattering ( $\epsilon \sim 1/4$ ) with no observable absorption from the QDs at this doping level [33, 34].

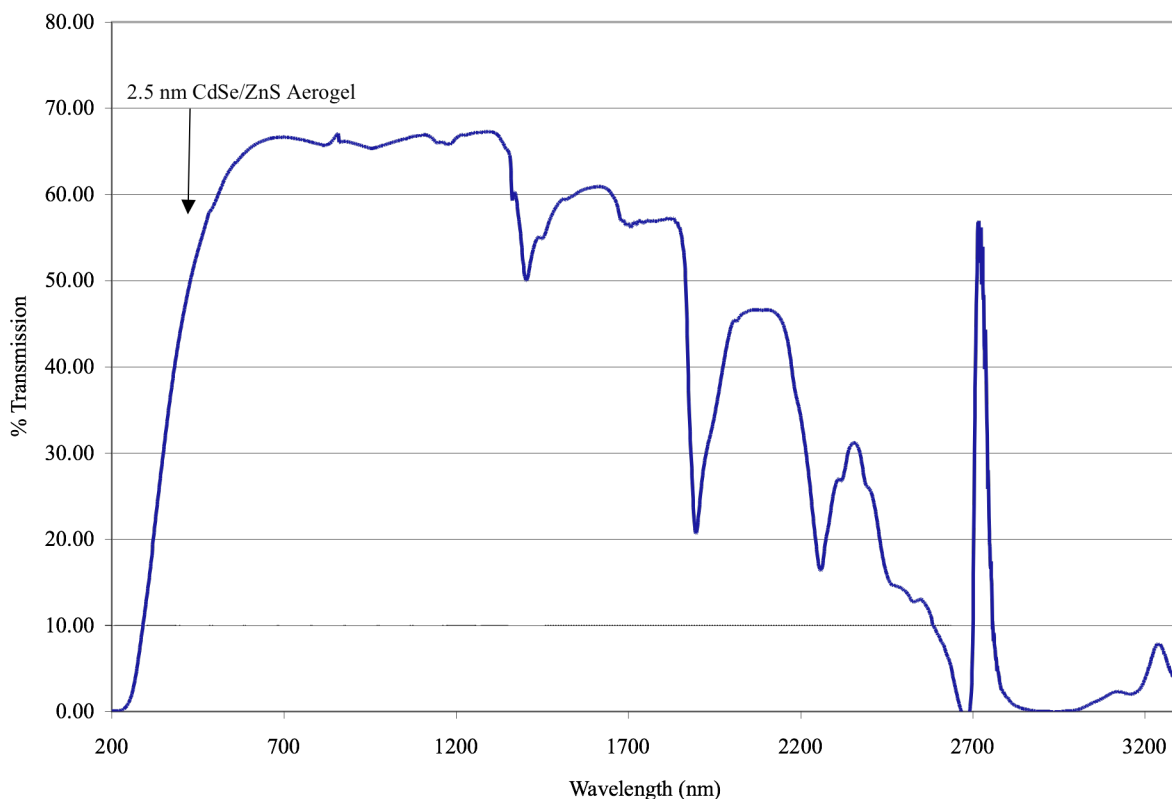


Figure 3.2 - UV-Vis scan of 2.5 nm CdSe/ZnS aerogel.

Using Yu's paper to determine the extinction coefficient of CdSe [35] as  $5.8989 \times 10^5$ , and with the absorbance from a UV-Vis scan of the red aerogel, we will be able to calculate concentration of CdSe/ZnS. Leaching of the QD through the multiple extraction processes necessary for aerogel formation was found to occur with the final materials containing less than the 1 mg of 2.5 nm CdSe per gram of aerogel used for synthesis. Notwithstanding the loss of some QD, the luminescent properties were excellent. As seen in Figure 3.3, QD doped aerogels show an intense green and red luminescence for the 2.5 and 6 nm QDs respectively. More importantly, as the figure indicates, the excitation beam penetrates deeply into the material with only moderate scattered by the medium. As a result the emitted light is observed to emerge from the length of the sample. This property is important for applications such as chemical sensing and for lasing and photonics.

The emission spectra of 2.5 and 6 nm QDs in solution and in the aerogel matrix is shown in Figure 5.4. The 6 nm dots, emitting in the red at  $\sim 620$  nm, is broader in the aerogel with a full-width-at-half-maximum of 57 nm compared to 48 nm for the same QD in solution. The emission maximum, however, is slightly shifted to the red in the aerogel. For the 2.5 nm dots, emitting in the green, those supported on the aerogel also exhibit a broader emission than they do in solution and, unlike the 2.5 nm dots, appear to have a markedly blue-shifted emission. While this may suggest that different sized dots interact differently with the silica surface, this conclusion may not be completely justified since the emission of the QD overlaps a relatively strong luminescence between 400-450 nm that arises from intrinsic chemical impurities (Sn and Ge) in the silica matrix [36]. As a result, the QD emission band is convoluted in such a way that it appears both broader and bluer shifted than it actually is. For application purposes, the supported QD must be robust and continue to emit over time. The materials described here appear to fit this criterion as no decline in emission intensity has been observed over a period of 5 months. This stability probably arises, at least in part, from the fact that in an aerogel the solvent has been completely removed, which limits solution phase bimolecular degradation processes.

In summary, the dispersion of luminescent CdSe QD in a low-density silica aerogel has been accomplished through the Sc CO<sub>2</sub> extraction of an alcogel containing the dissolved dots. The materials that result are robust and highly luminescent with good optical properties and extremely high surface area.



Figure 3.3 – 6 nm and 2.5 nm aerogels seen in room light and under 488 nm laser excitation as seen through a 488 nm filter. Luminescence seen in photo is from quantum dot emission.

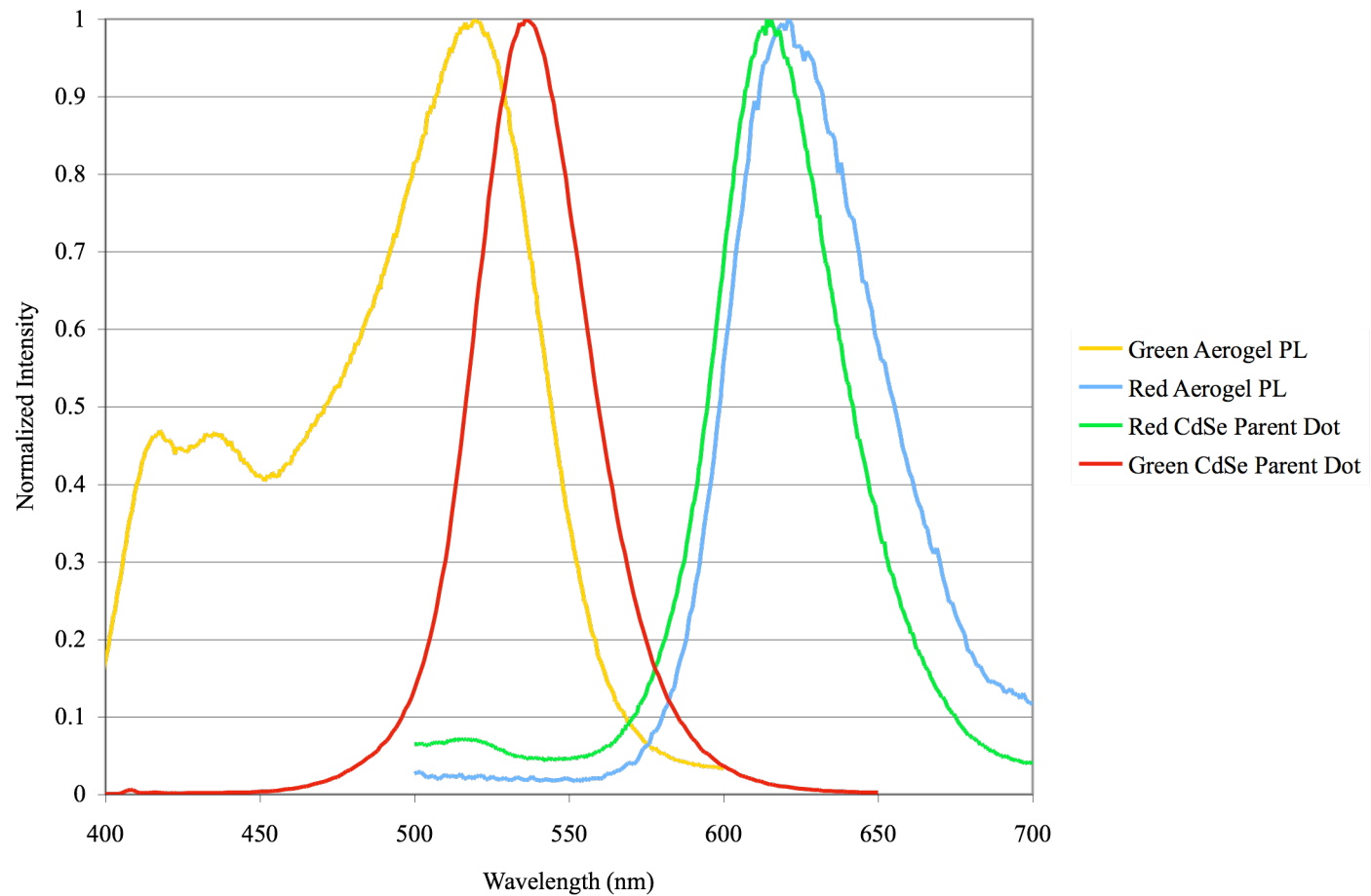


Figure 3.4 - Photoluminescence of 2.5 nm parent dot solution and aerogel (red and yellow) as well as 6 nm parent dot solution and aerogel (green and blue). Peaks at 420 nm are titanium impurity peaks from TMOS solution.

## CHAPTER 4

### CRITICAL POINT DRYING PROCEDURE FOR AEROGEL FORMATION

#### 4.1 Critical Point Drying

Critical point drying has extensively been used in the formation of silica aerogels. [37, 38] It is considerably safer than the alternative method of solvent extraction where the methanol or ethanol is taken to its critical point and then vented. Critical point drying is also used in the imaging of biological samples. A living tissue sample must be dry to view a sample using scanning electron microscopy. Letting tissue samples dry via normal evaporation or using a vacuum causes a distortion of the surface of the delicate cells. To circumvent this occurrence, the sample dried using a critical point dryer.

##### 4.1.1 Apparatus

SPI<sup>®</sup> Supplies manufactured the critical point drying cell used for this work [39]. It consists of water or alcohol cooled stainless steel jacket surrounding a pressured cavity, accessible at atmospheric pressure though the back. There is a viewing window in the front with a layer of safety Plexiglas covering it. The cell contains an inlet valve for the liquid solvent, a wash valve located on the bottom, a supercritical vent located on the top, and an overpressure safety valve, set at 2000 psi. Figure 4.1 shows the location of each of these valves.

##### 4.1.2 Supercritical Point

The critical point of any material is the point occurs when the temperature and pressure of a molecule is such that their gas and liquid phase are equal in density. Taking a liquid solvent past its critical point transforms the solvent to a condensed gas-like phase without any surface tension forces. That is to say that a sample submerged in a liquid which is then taken past its critical point will then be submerged in gas without ever being exposed to the damaging surface tension forces that can collapse delicate network structures. Above the critical point the gas

cannot be condensed to a liquid by changing the pressure only. The supercritical solvent can then be vented off. Figure 4.2 shows the phase diagram for carbon dioxide along with the temperature and pressure path taken to create our aerogels. The figure shows that by going around the critical point through supercritical fluid, damaging evaporative strains are avoided.

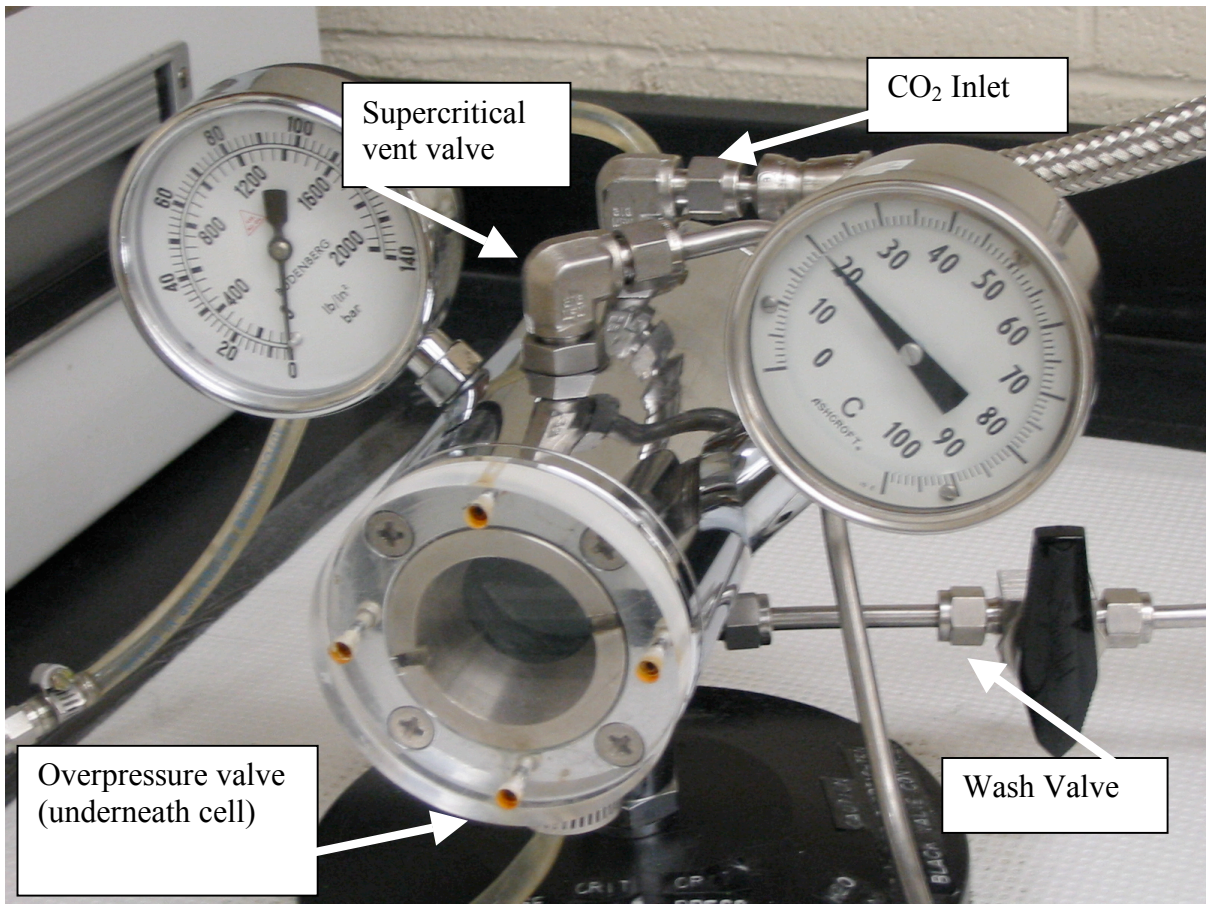


Figure 4.1 – Location of valves on critical point drying apparatus

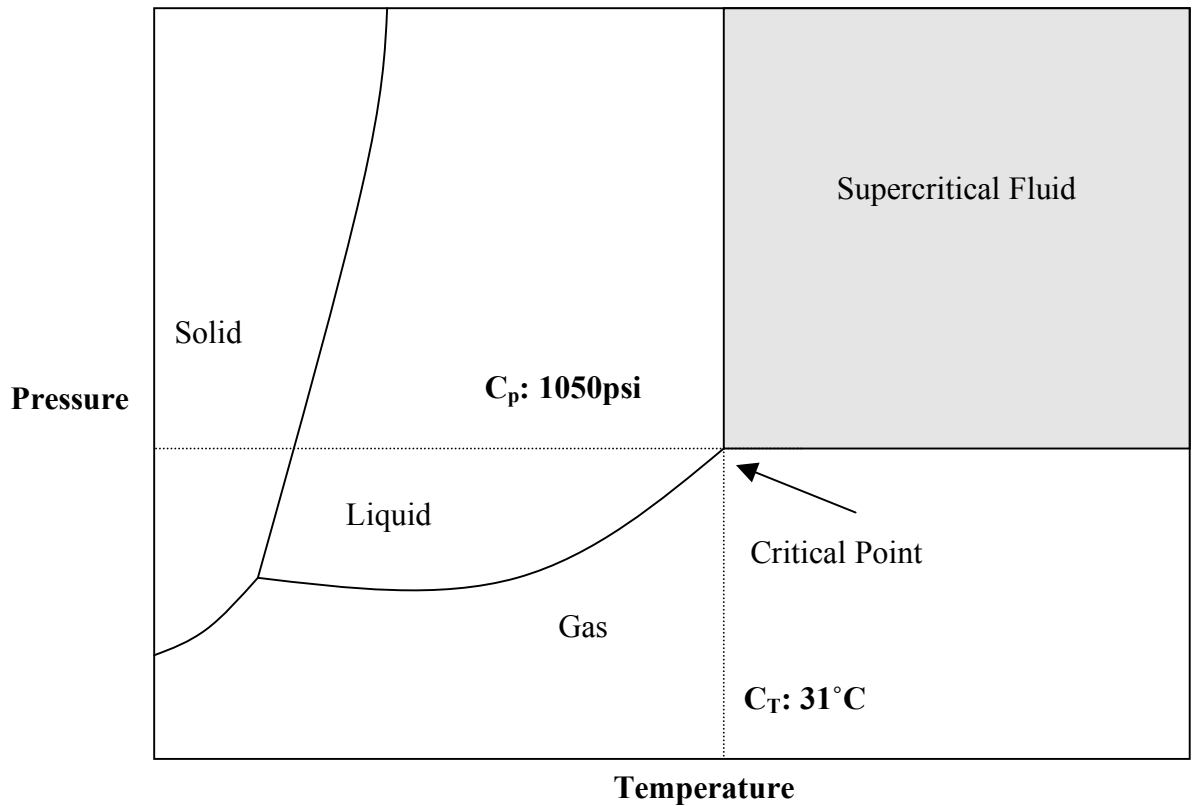


Figure 4.2 – Pressure-Temperature phase diagram for CO<sub>2</sub>

Supercritical fluid has also been used in chromatography and for solvent extractions for quite some time. Although it is not as popular as liquid or gas chromatography, it is well known for its solvating power [40]. Supercritical carbon dioxide is similar to pentane in polarity and apparent solvent strength [41].

Carbon dioxide is the most environmentally friendly solvent to use for this drying process but is not necessarily the most efficient. The company's website explains that using Freon as the solvent is more efficient for solvent exchange in samples. However, due to the environmentally degrading effects of Freon<sup>®</sup>113, it is difficult to obtain, cumbersome to use and dispose of properly.

#### 4.1.3 Solvent Exchange

The crucial step in critical point drying is to immerse the sample in the solvent that will be taken to the critical point. This may sound trivial but it is not. For example, water has a very

high critical point and is not easily displaced by liquid carbon dioxide. If the sample contains any water that has not been removed, the sample can be damaged during the drying process. When the initial sample solvent is not miscible with carbon dioxide, a solvent exchange must first be carried out. This can be achieved through a single or multiple step process.

For our procedures, the formed aerogel was aged in a water/methanol solution that was approximately equivalent to the composition of the formation concentration for a period of 24 hours. This solution was then replaced with dry methanol and a light vacuum was pulled on the closed container. Subsequent washes were completed every few hours with dry methanol until I was reasonably confident that all the water had been removed from the aerogel. For a 1 cm x 1 cm x 5 cm aerogel, approximately 10 washes were completed over the course of three days with the latter washes sitting for longer times.

I also experimented with using a two-step solvent extraction going through methanol and to acetone. This extraction takes place by first aging the aerogel in a solvent that is the same make-up of the formed aerogel, usually a 20 to 1 ratio of methanol to water. The next wash is made up of only methanol followed by a 1:1 mix of methanol to reagent grade acetone. Subsequent washes are 100% acetone and are longer in duration. Carbon dioxide is more miscible with acetone than methanol and the solvent exchange that occurs in the supercritical cell therefore is more complete. The aerogels that are produced through acetone washing are very high in quality.

## **4.2 Instrument Use**

### **4.2.1 Turning on Instrument**

The first step is to place the sample in the cell along with the final volume of dry wash that it was submerged in. Tip the cell forward and gently sliding the sample in along with the wash. Screw the back of the cell chamber in place and gently tighten. Open the gas cylinder and pressurize the cell with approximately 750 psi. When the liquid CO<sub>2</sub> tank is running low, the critical point can be reached as long as the pressure is above 650 psi. To turn on the instrument is to insure that the coolant reservoir is filled with isopropanol (Figure 4.3, Step 1.) Once filled, to mark indicated on instrument, turn on both the main switch and the cooling switch (Figure 4.3, Step 2 and 3 respectively.) Depress the 'Set In/Read Out' button and dial the temperature with the 'Temperature Set' button (Figure 4.3, Step 4.) Set temperature to 2°C. Return to instrument



in twenty minutes to read temperature, check to see that the cell is full of liquid, and begin the venting stage.

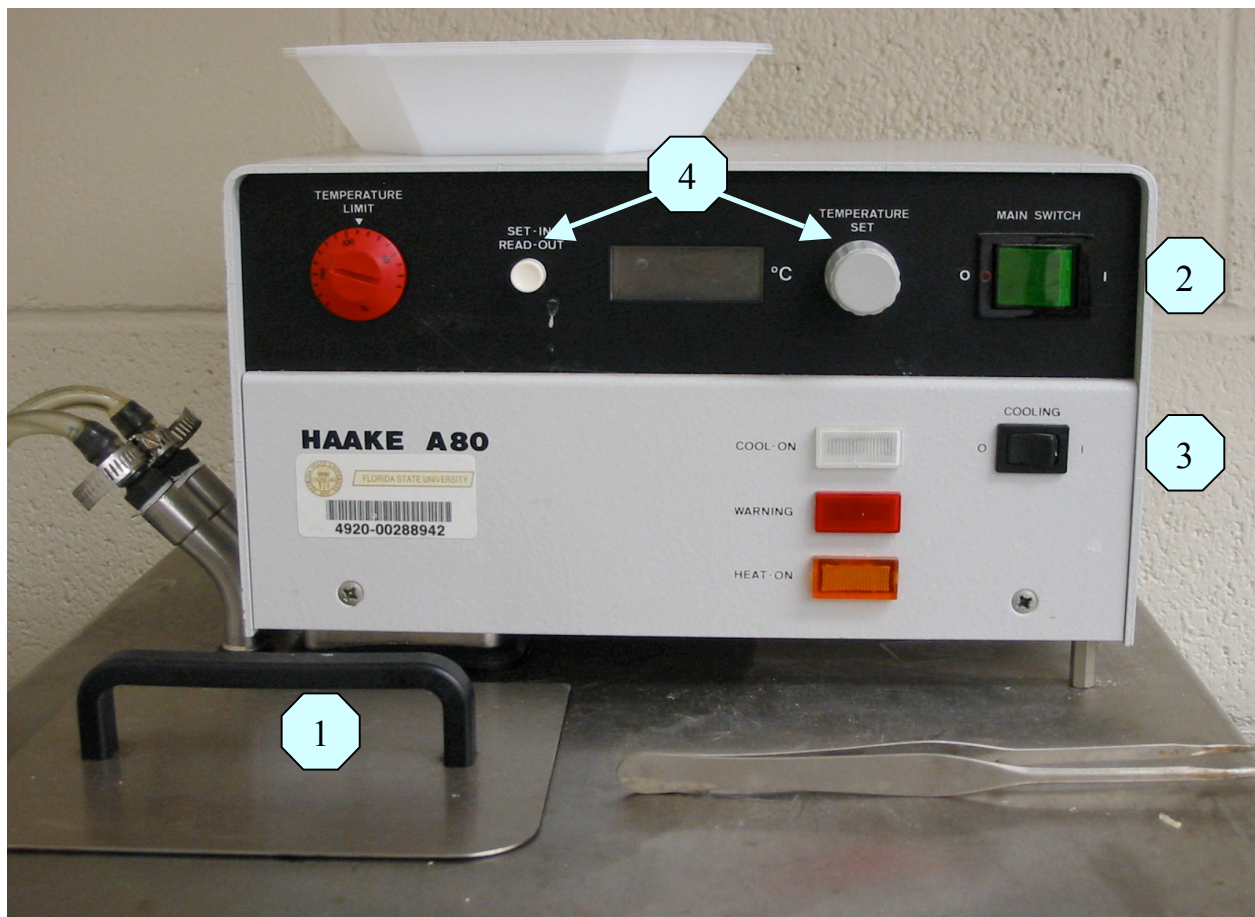


Figure 4.3 – Coolant control box of critical point dryer

#### 4.2.2 Venting and Supercritical Stages

Once the cell is filled with liquid, venting can begin. A catch beaker is necessary during the first few washes to capture the methanol or acetone. The duration and repetition of venting and washes will depend on each individual sample. The sample should never be allowed to be dry in the cell for any length of time.

Once the sample has been adequately washed, slightly open the supercritical vent valve to make sure it doesn't have any methanol/acetone remaining within it. Close all valves, including the valves to the gas cylinder. Set temperature of 2-propanol to 40°C and turn off the 'cooling' switch. Stay with apparatus and vent cell using supercritical vent if the pressure rises above 1150-1200 psi. Once the temperature of the cell is 35°C and the pressure is 1100 psi you have reached the critical point of CO<sub>2</sub>. Keep the cell at 35°C while venting to insure that condensation of gas does not occur. Let the cell remain at this temperature and pressure for a few minutes. Very slowly vent the cell back down to atmospheric pressure. Ideally, the vent should take about an hour. Once cell is back down to atmospheric pressure, turn off the instrument and open the cell to view the aerogel.

#### **4.2.3 Problem Solving**

Supercritical carbon dioxide is used as a solvent in chromatography. At its supercritical point, carbon dioxide has the same solubility as hexane. Any organic components of the aerogel that are not chemically bound to the silica can be washed out with the vent waste. Cracking, shrinking, or peeling of the aerogel sample after it has gone through the critical point dryer is indicative of incomplete drying or a poorly formed alcogel.

## CHAPTER 5

### PRIMITIVE SENSOR EXPERIMENTS

#### **5.1 Sensor Introduction**

With societal and political unrest making news headlines, there is an obvious need for accurate detection of materials that are capable of casualty; detection of explosives included. Explosive materials cause significant damage to life and property and as such are high priorities of world governments to create accurate and precise detection. The problem of detection is as old as explosives themselves. Currently, only trained canines have been able to reliably and inexpensively search large areas and detect explosives through sniffing the air [42]. There is considerable interest in the development of an electronic nose that is as sensitive and reliable as a dog while being more robust and less expensive.

##### **5.1.1 Electronic Noses**

The main challenge to explosive sensor technology is the inherently low vapor pressure of explosive materials. Trinitrotoluene (TNT) has a vapor pressure of 7 ppb at room temperature under ideal conditions [43, 44]. The vapor pressure of RDX and HMX are less than that of TNT. These detection limits can drop drastically once atmospheric contaminants are introduced. The requirement for an electronic nose or sensor is that it be small, portable, sensitive, and low cost. The instrument should have low false alarm rates as well. Current explosive sensor technologies include amplifying fluorescent polymers [45], micro-machined cantilevers that detect adsorption [46], chemiluminescence [47], and conductive carbon nanotubes [48]. Each technology has its strengths and weaknesses, and there is still an opportunity for a parallel or alternative technologies.

##### **5.1.2 Nanomaterials as Environmental Sensors**

The increased interest in nanomaterials has produced research using these materials as sensors for various analytes [49]. They are useful for real-time monitoring of a vast number of

analytes. Luminescence-based or absorbance-based sensors can be very sensitive to small changes in concentration of a target compound. The nanomaterial can be tailored via capping surface ligands to be chemically selective for a certain material and thus the material can be detected through a change in luminescence or absorbance.

The original focus of embedding quantum dots in a silica matrix was to place these highly sensitive chemical sensors in a medium for easy detection. To synthesize a responsive quantum dot sensor required that the preferred target material be able to reversibly bind to the surface of the ligand and quickly create a drop in the luminescent properties by acting as an electron acceptor in a non-radiative energy transfer event. The preliminary results of this study show that CdSe quantum dots do not perform as desired as chemical sensors to explosive vapors.

## **5.2 CdSe Response to TNT**

### **5.2.1 CdSe on Alumina Filter**

To perform the preliminary sensor capability of CdSe quantum dots to various explosive vapors, the CdSe had to be suspended in a matrix that was easy to detect changes in luminescence from vapors. We decided a simple way to go about this was to filter a colloidal solution of CdSe onto filter paper. Using an alumina-based 0.02  $\mu\text{m}$  pore Whatman Anodisc™ 47 mm diameter filter paper, I pulled through a solution containing a small amount of CdSe dots that had not been core-shelled with ZnS. The amount weight deposited to the disks was approximately 10 mg. The solvent was allowed to dry off of the disks before taking front-face luminescence. The 6 nm CdSe dots were excited at a wavelength of 400 nm using 2.5 mm slits. Since I was not certain that the layer of CdSe was homogenous, the disks were rotated and multiple points sampled for average excitation intensity. The disk was then crudely exposed to TNT vapors by placing the disk in a beaker with an opened bottle of TNT crystals, taking care not to let the bottle touch the disk. The beaker was covered and after 45 minutes of exposure, the luminescence of the disk was re-run. The disk was then placed in an oven and heated to 200°C to volatilize the TNT off of the sample and once cooled, the luminescence was taken for a third time. The results of this run can be seen in Figure 5.1. Error bars can be seen on this figure extending from the average of four luminescence measurements.

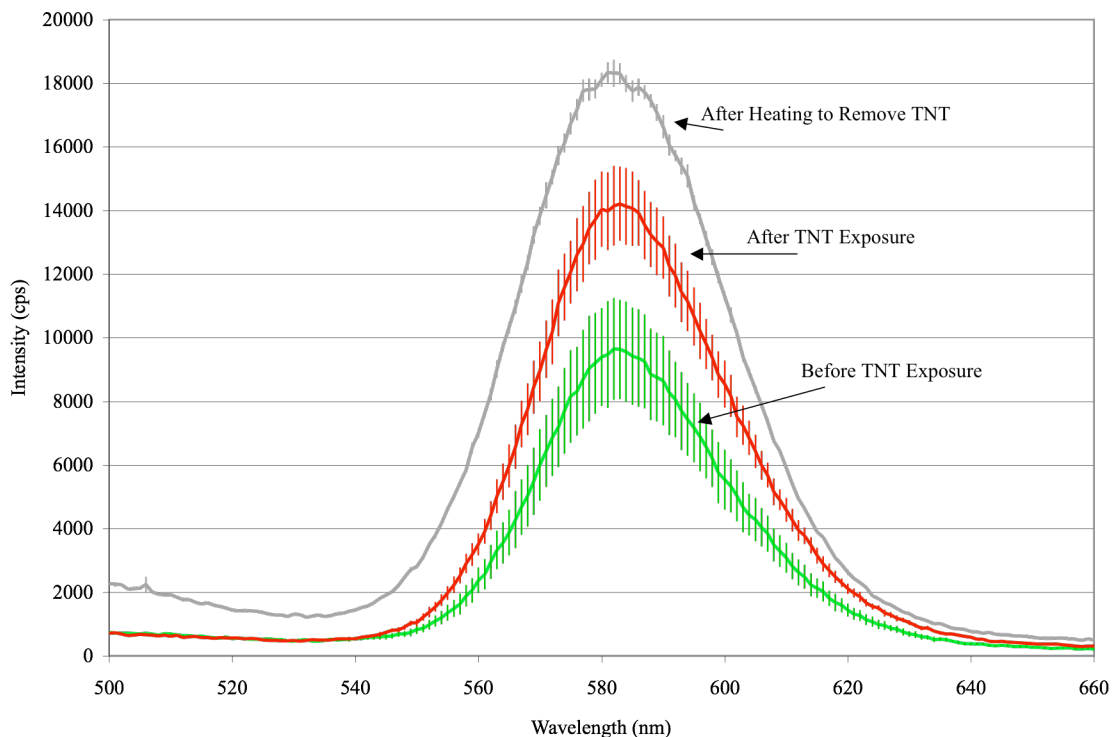


Figure 5.1- Photoluminescence of 6 nm CdSe dots before and after TNT exposure and also after heating to remove TNT.

The figure shows that the CdSe luminescence was not quenched by the TNT exposure, as expected, but enhanced. Once more, after heating the sample luminescence was again enhanced.

This experiment was repeated using 3 nm CdSe and 3 nm CdSe/ZnS with similar results. Each showed an enhancement of luminescence after TNT exposure with the CdSe/ZnS sample having the smallest percent change in luminescence. One interesting observation, after measurements had been taken and the Anodisc was held under a UV hand lamp, the pattern from excitation could be seen as a ‘ghost image.’ This ‘ghost image’ faded after a day of sitting on a lab bench. It is unknown how this image affected the luminescent results from the experiment.

### 5.2.2 CdSe in Xerogels

Fractured portions of xerogel unfit for further spectroscopic studies were placed in contact to TNT vapors to access approximate response. Xerogels are not the preferred medium for gas phase sensor work because their inherent low porosity, generally around 3 nm, hinders rapid gas diffusion and therefore would make for slow response times. We chose them because they were leftovers from previous experiments and gave a good indication of approximate

response. Xerogel pieces were placed in a test tube, covered with a loose wad of cotton and TNT was placed on top. The test tube was then covered and TNT vapors were allowed to come to equilibrium in the test tube.

The results were not sufficient enough to produce any conclusions but we made several observations. The volatile solvents that were still coming off of the xerogel samples interacted with the TNT, changing the color of the solid TNT sample from off-white to yellow. Likewise, the TNT vapors turned the clear to white xerogels to orange in color. The luminescence of the samples did drop off but with the information from the previous study and the drastic color change of both samples indicate that a chemical changes were occurring that may have affected the luminescence, not the sensing of TNT vapors.

### **5.3 Recommendations for Further Explosive Sensor Research**

If experimentation is to be continued into the possibility of quantum dots to be used as a gas-phase sensor of explosive threats, the phenomena of brightening will need to be addressed. Also, for maximum selectivity, a target ligand should be selected for its affinity to bind to the target molecule. An example of this work can be seen in the literature as a solution-based sensor [50].

## CHAPTER 6

### CONCLUSIONS

#### **6.1 Unanswered Questions**

Since my time here was very limited due to the nature of my exchange program, I could not get to all the interesting science that popped up along my journey. The goal of this chapter is to direct a future graduate student interested in this work as to where this work finished and questions left to be answered.

##### **6.1.1 Xerogel**

There is much work to be done in the area of reproducible and consistently performing sol formation. As was mentioned in Chapter 2, these gels seemed to have a ‘mind of their own’ and turn on, off, cloud, clear, and crack with little known reason or rhyme. I attempted to make sense out of these observations but could not find a direct correlation between any of the events. General observations were that gels seemed to go through a cloudy/clear transition during significant changes in ambient temperature and humidity. However, this could not always be reproduced in a laboratory setting. Gentle heating to 50°C or placement in a dry box would make cloudy samples clear. Serial samples created with varying HDA and APeS concentration did not yield successful results as the monoliths cracked and were not uniform. This set of experiments should be repeated with greater care to attempt to explain the cloudy gels.

Although I almost exclusively worked with TMOS, there is good indication that TEOS samples may give just as good of results. A series of ligands and dot sizes should be combined to explore more options for material synthesis.

##### **6.1.2 Aerogel**

The aerogel work I completed was by far the more interesting aspect of my research and by far took the most time to get to work. I did not do all the material studies that I would have liked such as accurately measuring the quantum dot concentration, the quantum dot stability, and

altering the aerogel density, to name a few. It took quite a bit of trial and error to get the aerogels to work in the first place and it would be very interesting to do spectroscopic studies on this fascinating material.

### **6.1.3 Sensors**

Explosive sensor background literature searching was very interesting and I learned a significant amount about what the state-of-the-art is currently. The sensor work unfortunately fell by the wayside as we found that the dots behaved in a manner that was not expected. For quantum dot sensor work to be viable and competitive on the current market, it would have to show a vast improvement over existing technology. The best answer to the search for sensor material would be an on/off signal that was tuned to specific targets. Since the real world environment is much more contaminated and more difficult to predict than laboratory studies, detector development would not be a trivial task to take on. Nonetheless, its importance is paramount if it could make a significant difference.

## **6.2 Conclusions**

I leave FSU with a research project with more questions to be answered than it seems with which I started. We have produced stable, highly luminescent silica xerogels embedded with semiconducting quantum dots as well as optically clear aerogels with visible luminescence from embedded quantum dots. These materials are stable for several months and can accommodate a range of sizes of quantum dots. Preliminary sensors work shows an unexpected brightening of CdSe upon exposure to TNT vapors. This research opens the door to the combination of two very different materials research branches into a platform for future breakthroughs in lighting, optical, or sensors.



## REFERENCES

- [1] Clarkson, T.W. *Journal of Trace Elements in Experimental Medicine*, **1998**, *11* (2-3), 303-317.
- [2] Bhargava, R. N.; Chhabra, V.; Som, T., Ekimov, A.; and Taskar, N.; *Phys. Stat. Sol. (b)*, **2001**, *229*, No. 2, 897 – 901.
- [3] Shatalov M.; Chitnis, A.; Adivarahan, V.; Lunev, A.; Zhang, J.; Yang, J.W.; Fareed, Q.; Simin, G.; Zakheim, A.; Asif Kahn, M.; Gaska, R.; Shur, M.S.; *Appl. Phys. Lett*, **2001**, *78* (6), 817-819.
- [4] Mangolini L.; Thimsen E.; Kortshagen U.; *Nano Letters*, **2005**, *5* (4), 655-659.
- [5] Narendran, N.; *Physics World*, **2005**, *18* (7), 25-29.
- [6] Murphy, C. J.; Coffey, J. L.; *Applied Spectroscopy*, **2002**, *56* (1), 16A-27A.
- [7] International Society for Optical Engineering. *Sol-Gel Optics*, Vol 1328; San Diego, CA, 1990.
- [8] Spanhel, L.; Haase, M.; Weller, H.; and Henglein, A.; *J. Am. Chem. Soc.*, **1987**, *109*, 5649.
- [9] Selvan, S. T.; Bullen, C.; Ashokkumar, M.; Mulvaney, P.; *Adv. Mater.* **2001**, *13*, 985-988.
- [10] Wang, Q.; Iancu, N.; Seo, D. K.; *Chem. Mater*, **2005**, *17*, 4762-4764.
- [11] Correa-Duarte, M.A.; Kobayashi, Y.; Caruso, R.; Liz-Marzan, L.M.; *J. Nanosci. Nanotechnol*, **2001**, *1*, 95.
- [12] Correa-Duarte, M.A.; Giersig, M.; Liz-Marzan, L. M.; *Chem. Phys. Lett.* **1998**, *286*, 497.
- [13] Murase, N.; Yang, P.; Li, C. L.; *J. Phys. Chem. B.*, **2005**, *109*, 17855-17860.
- [14] Li, C. L.; Ando, M.; Murase, N.; *Phys. Stat. Sol (c)*, **2003**, *4*, 1250-1253.
- [15] Mohanan, J. L.; Arachchige, I. U.; Brock, S. L., *Science*, **2005**, *307*, 397-400.

- [16] Lawrence Berkeley National Laboratory. *Silica Aerogels*.  
<http://eande.lbl.gov/ECS/aerogels/satoc.htm> (accessed 31 May 2005).
- [17] Gerbec, J. A., Magana, D., Washington, A., Strouse, G.F., *J. Am. Chem. Soc.*, (2005), ASAP Article.
- [18] Li, J. J.; Wang, Y. A.; Guo, W.; Keay, J. C.; Mishima, T. D.; Johnson, M. B.; Peng, X., *J. Am. Chem. Soc.*; **2003**; *125*(41); 12567-12575.
- [19] Soult, A. S.; Carter, D. F.; Schreiber, H. D.; van de Burgt, L. J.; Stiegman, A. E.; *J. Phys. Chem. B.*; **2002**; *106*(36); 9266-9273.
- [20] Alivisatos, A. P.; *Science*, **1996**, *271*, 933.
- [21] Potter, B. G.; Simmons, J. H.; *Phys. Rev. B*, **1988**, *37*, 10838.
- [22] Jain, R. K.; Lind, R. C.; *J. Opt. Soc. Am.*, **1983**, *73*, 647.
- [23] Li, Y.; E. Liu, C. Y.; Pickett, N.; Skabara, P. J.; Cummins, S. S.; Ryley, S.; Sutherland, A. J.; O'Brien, P.; *J. Mater. Chem.* **2005**, *15*, 1238.
- [24] Olsson, Y. K.; Chen, G.; Rapaport, R.; Fuchs, D. T.; Sundar, V. C.; Steckel, J. S.; Bawendi, M. G.; Aharoni, A.; Banin, U.; *Appl. Phys. Lett.*, **2004**, *85*, 4469.
- [25] Javier, A.; Meulenberg, R. W.; Yun, C. S.; Strouse, G. F.; *J. Phys. Chem. B*, **2005**, *109*, 6999.
- [26] Walker, G. W.; Sundar, V. C.; Rudzinski, C. M.; Wun, A. W.; Bawendi, M. G. D.; Nocera, G.; *Appl. Phys. Lett.*, **2003**, *83*, 3555.
- [27] Selvan, S. T.; Bullen, C., Ashokkumar, M.; Mulvaney, P., *Adv. Mater.*, **2001**, *13*, 985.
- [28] Wang, Q. B.; Iancu, N.; Seo, D. K.; *Chem. Mater.*, **2005**, *17*, 4762.
- [29] Gerbec, J. A.; Magana, D.; Washington, A.; Strouse, G. F.; *J. Am. Chem. Soc.*, **2005**, *127*, 15791.
- [30] Li, J. J.; Wang, Y. A., Guo, W. Z; Keay, J. C.; Mishima, T. D.; Johnson, M. B.; Peng, X. G.; *J. Am. Chem. Soc.*, **2003**, *125*, 12567.
- [31] Brinker, C. J.; Scherer, G. W.; *J. Non-Cryst. Solids*, **1985**, *70*, 301.
- [32] Emmerling, A.; Petricevic, R.; Beck, A.; Wang, P.; Scheller, H.; Fricke, J.; *J. Non-Cryst. Solids*, **1995**, *185*, 240.
- [33] Beck, A.; Gelsen, O.; Wang, P.; Fricke, J.; *Journal De Physique* **1989**, *50*, C4203.

- [34] Beck, A.; Caps, R.; Fricke, J.; *J. Phys. D-Appl. Phys.*, **1989**, 22, 730.
- [35] Yu, W., Lianhua, Q., Guo, W., Peng, X., *Chem. Mater*, **2005**, 15, 2854-2860.
- [36] Soult, A.; Carter, S. D. F.; Schreiber, H. D.; van de Burgt, L. J.; Stiegman, A. E.; *J. Phys. Chem. B*. **2002**, 106, 9266.
- [37] Hua, D.W., Anderson, J., Di Gregorio, J., Smith, D.M., Beaucage, G., *J. Non-Cryst. Solids*, **1995**, 186, 142-148.
- [38] Land, V.D., Harris, T.M., Teeters, D.C., *J. Non-Cryst Solids*, **2001**, 1-3, 11-17.
- [39] SPI® Supplies, *Critical Point Dryers Technique*, [http://www.2spi.com/catalog/instruments/dryers\\_technique.html](http://www.2spi.com/catalog/instruments/dryers_technique.html) (accessed 1 November 2005.)
- [40] Smith, R.M., *J. Chromatogr. A.*, **1999**, 856, 83-115.
- [41] Berger, T. A. *J. Chromatogr. A* **1997**, 785, 3-33.
- [42] Vapour and Trace Detection of Explosives for Anti-Terrorism Purposes: M. Krausa, A. Reznev, eds.; NATO Science Series II: Mathematics, Physics and Chemistry; Kluwer; The Netherlands, 2004; Vol. 167.
- [43] Electronic Noses and Sensors for the Detection of Explosives; J. Gardner, J. Yinon, eds.; NATO Science Series II: Mathematics, Physics and Chemistry; Kluwer: The Netherlands, 2004; Vol. 159, pp 302-303.
- [44] Jenkins, T., Leggett, D., Miyares, P., Walsh, M., Ranney, T., Cragin, J., George, V., *Talanta*, **2001**, 54, 501-513.
- [45] Yang, J., Swager, T., *J. Am. Chem. Soc.*, **1998**, 120, 1184-11873.
- [46] Pinnaduwaige, L., Wig, A., Hedden, D., Gehl, A., Yi, D., Thundat, T., Lareau, R., *J. Appl. Phys.*, **2004**, 95 (10), 5871-5873.
- [47] Sohn, H., Calhoun, R., Sailor, M., Trogler, W., *Angew. Chem. Int. Ed.*, **2001**, 40 (10), 2104-2105.
- [48] Moore, D. S., **2004**, *Rev. Sci. Instrum.*, 75 (8), 2499-2508.
- [49] Shi, J., Zhu, Y., Zhang, X., Baeyens, W., Garcia-Campana, A., *Trends in Anal. Chem.*, **2004**, 23 (5), 351-360.
- [50] Goldman, E., Medintz, I., Whitley, J., Hayhurst, A., Clapp, A., Uyeda, H., Dechamps, J., Lassman, M., Mattoussi, H., *J. Am. Chem. Soc.*, **2005**, 127 (18), 6744-6751.

## BIOGRAPHICAL SKETCH

### **Lindsey M. Wolf Sorensen**

Lindsey M. Sorensen was born September 28<sup>th</sup>, 1979 in the town of Tonawanda, NY. She graduated with honors from Springville Griffith Institute High School in 1997. Lindsey graduated Magna Cum Laude with a Bachelors of Science degree, with honors, from Chatham College, Pittsburgh, PA in 2001. She was a distinguished graduate of ROTC and was commissioned in May of 2001 as an officer in the United States Air Force.

Her first active duty assignment was as Program Manager for the Atmospheric Threat Protection Group at the Air Force Research Laboratory, Materials and Manufacturing Directorate, Airbase Technologies Division, Tyndall AFB, Florida. She was selected to attend Florida State as an Air Force Institute of Technology Civilian Institute program student. Lindsey was promoted to the rank of Captain while attending FSU and her next assignment is as Chief of Aerospace Fuels Laboratory, RAF Mildenhall, United Kingdom. Lindsey is married and has two dogs.